University of Alberta

A Novel Synthetic Route Towards Conjugated Polymers for Photovoltaic Materials via Metallacycle Transfer

by

Le Kang

A thesis submitted to the Faculty of Graduate Studies and Research
in partial fulfillment of the requirements for the degree of

Master of Science

Department of Chemistry

©Le Kang
Fall 2012
Edmonton, Alberta, Canada

Abstract

Conjugated polymers are actively studied as photovoltaic materials in bulk heterojunction solar cell devices. Five-membered heterocycles, typically thiophene and its derivatives, are the most common building units in these polymers. However, conjugated polymers containing inorganic elements other than sulfur have received less research attention due to associated synthetic difficulties, even though incorporation of main group elements (such as selenium) has led to improved power conversion efficiency relative to thiophene-based polymers. Zirconium-mediated metallacycle transfer chemistry developed by Fagan *et al.* provides an easy access to obtain a series of main group heterocycles. Our goal is to apply this metallacycle transfer chemistry towards polymer synthesis and develop a synthetic route to prepare polymers whose band gaps can be tunable by incorporating various main group elements. The work described in this Thesis involves the use of metallacycle transfer chemistry to prepare conjugated hybrid thiophene-selenophene polymers for future application as photovoltaic materials.

Table of Contents

Chapter 2. Synthesis of Conjugated Polymers via Zirconium-Mediated Metallacycle Transfer Chemistry

Chapter 3. Summary and Future Work

List of Tables

List of Figures

List of Schemes

List of symbols, nomenclature and abbreviations

Ar: Aryl group

BHJSC: Bulk Heterojunction Solar Cell

Bpin: 4,4,5,5-tetramethyl-1,3,2-dioxaborolate

Bu: Butyl group

COD:1,5-cyclooctadiene

Cp: Cyclopentadienyl

EI: Electron Ionizaiton

EQE: External Quantum Efficiency

Et: Ethyl group

eV: Electron-volt

FF: Fill Factor

GPC: Gel Permeation Chromatography

HOMO: Highest Occupied Molecular Orbital

HR-MS: High Resolution Mass Spectroscopy

I_{op}: Output current

^{i}Pr: Isopropyl group

I_{sc}: Short circuit current

ITO: Indium tin oxide

LUMO: Lowest Unoccupied Molecular Orbital

MALDI: Matrix-assisted Laser Desorption/ionization

Me: Methyl group

NBS: *N*-Bromosuccinimide

NMR: Nuclear Magnetic Resonance

P3HS: Poly-3-hexylthiophene

P3HT: Poly-3-hexylselenophene

PBSC: Polymer-based Solar Cell

PCBM: [6,6]-Phenyl-C_{61}-butyric acid methyl ester

PDI: Polydispersity Index

PCE: Power Conversion Efficiency

Ph: Phenyl group

P_{in}: Power input

PV: Photovoltaic

TGA: Thermogravimetric Analysis

THF: Tetrahydrofuran

UV-vis: Ultraviolet-visible spectroscopy

V_{oc}: Open circuit voltage

V_{op}: Output voltage

α, β, γ: Unit cell angles

λ_{max}: Maximal absorbance wavelength

ρ: Density

Chapter 1: Introduction

1.1 Introduction to photovoltaic materials

The urgent need to develop environmentally friendly, renewable, sources of energy in order to meet the rapid growth in energy demand is one of the biggest challenges in the new century. Amongst the many promising renewable energy sources, the bright prospect of solar photovoltaic (PV) power is widely recognized; consequently, the solar cell industry has emerged to become the fastest growing power-generation method in the last five years (Figure 1.1)[1]
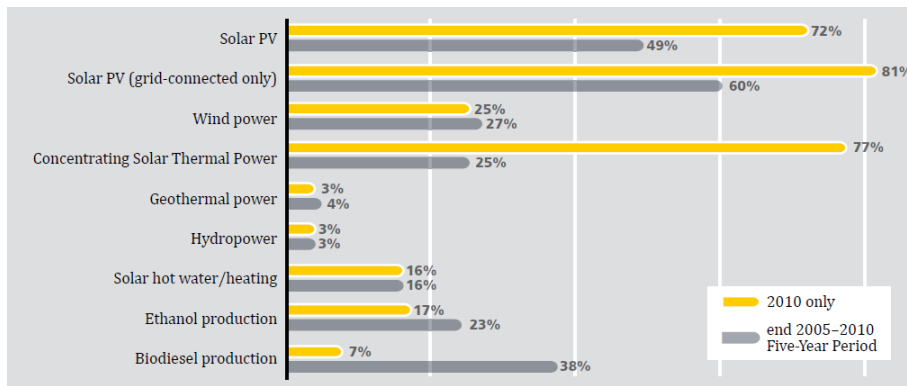
Figure 1.1 Average annual growth rates of renewable energy from 2005–2010.[1]

Currently, over 85% of the photovoltaic materials manufactured annually involve inorganic materials, such as silicon, gallium-arsenide (GaAs), cadmium telluride (CdTe), and cadmium-indium-selenide (CIS).[2] However, the solar energy share of the global total energy production was still less than 0.5% in 2009 because there are a few significant drawbacks that keep the current inorganic solar cells from adopting a leading role in the energy market. For example, the major obstacle to the widespread production of silicon-based solar cells is their expensive production costs due to the requirements of very pure,

1

solar-grade, silicon (usually greater than 99.999%).[3] Large silicon panels are also very heavy and mechanically inflexible, which limit their application in many fields.

During the past decade, a new type of PV material, conjugated polymer-based solar cells, has been actively investigated. Polymer-based solar cells (PBSCs) possess exceptional advantages as compared to the crystalline silicon solar cells. For instance, most conjugated polymers used in PBSC devices have solubilizing groups present and hence dissolve in common organic solvents. The high solubility of those materials make them compatible with large-scale processing methods such as thin film printing technologies.[4] Mass roll-to-roll production of devices is also achievable due to the flexibility and lightweight nature of PV polymers.[5] Those advantages give PBSC the possibility to compete with inorganic PV materials in future energy generation markets.

1.1.1 Working principles of polymer-based solar cells (PBSCs)

The development of conjugated polymers for applications in electronics as PV materials started in 1977.[6] A major breakthrough was achieved by Tang in 1986, when a power conversion efficiency (PCE) of 1% was reported for a polymeric solar cell by bringing a polymeric electron donor and a molecular electron acceptor together in a single device.[7] Even though the PCE obtained was still too low for practical applications, the heterojunction concept introduced in their studies has been widely employed in subsequent architectures of PV cells with great success. To date, extensive progress has been achieved in understanding how the structure of the materials and device design controls the performance of polymer-based PV materials. We will use the heterojunction

device arrangement in Figure 1.2 (b) to explain the components of a polymer-based PV device and its working principles.
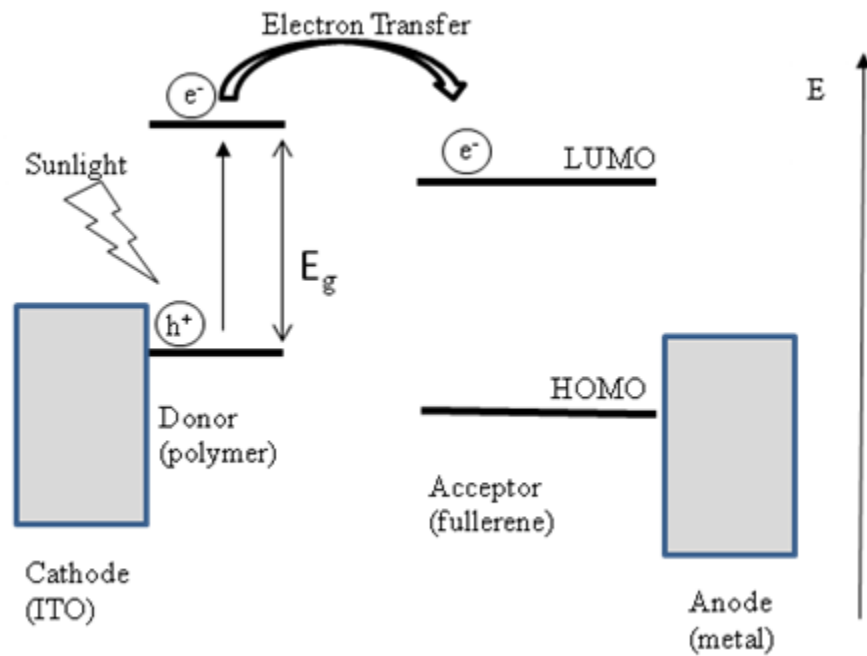
(a)
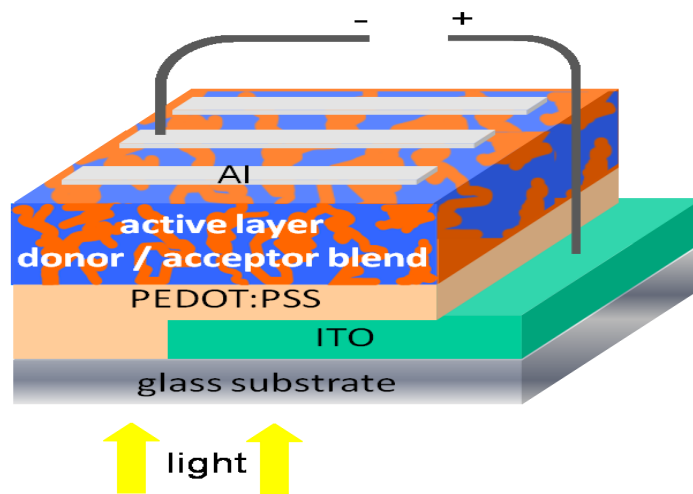
(b)

Figure 1.2 (a) Schematic drawing of the working principles behind polymer solar cells (b) Cross-section of bulk heterojunction polymer solar cells.[5]

When a functional PV device converts solar energy to electricity, the following four steps must occur: (1) absorption of light to give an electron-hole pair (exciton); (2) charge transfer and separation of opposite charges; (3) charge transport; (4) charge collection.[8]

Photovoltaic cell configurations based on organic materials differ from those based on inorganic Si semiconductors because the physical properties of inorganic and organic materials are significantly different. Generally, inorganic semiconductors have high dielectric constants and low exciton (created by absorption of photons) binding energies, implying higher charge mobility and ease of charge separation. Specifically, room temperature can provide enough thermal energy to dissociate the exciton into a positive and negative charge carrier, and the resulting electrons and holes are easily transported due to high mobility of the charge carriers.

Conversely, polymer-based PV materials generally have low dielectric constants and high exciton binding energies, which make separation of excitons relatively more difficult than in inorganic PV materials; thus, separation of excitons into free charge carriers does not readily occur at room temperature. Therefore, the electron donor-acceptor concept in heterojunction architecture is the current solution to overcome the problem. The photovoltaic polymer that makes up the electron donor layers first absorbs sunlight which excites electrons from its valence band (HOMO) to its conduction band (LUMO) which, in turn, creates an exciton, an electrostatically bounded electron-hole pair ($e^- $-$h^+$).

Separation of the exciton is a key step in generating electricity within a PV device. There are several competing steps in the form of electron relaxation which can occur in

place of charge separation. The Jablonski diagram (Figure 1.3) describes the phenomena of fluorescence and phosphorescence which can both lead to reduction in the amount of solar energy that is converted into electricity energy. When an electron is excited from a singlet ground state S_0 to higher singlet energy state (S_1, S_2 etc), non-rediactive transitions may occur between higher energy states. The two pathways of electron relaxation that lead to light emission are fluorescence and phosphorescence. Fluorescence occurs by a direct relaxation of electrons from a higher energy state to the ground energy state and the lifetime of this process is an nanosecond scale. On the other hand, phosphorescence involves intersystem crossing between higher singlet energy state (S_1) and triplet energy state (T_1). Relaxation of the electron from the triplet state to a singlet state is much slower due to the requirement of a kinetically unfavored electron spin flip (thuse the lifetime are in the millisecond range).
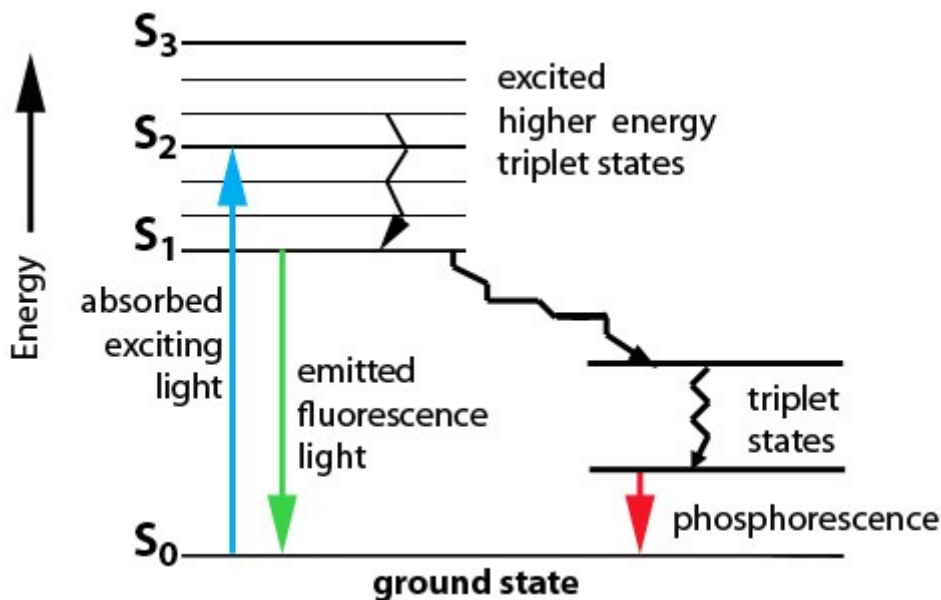
Figure 1.3 Jablonski diagram for process of fluorescence and phosphorescence.

In order to minimize fluorescence and phosphorescence, acceptor materials (usually fullerene derivatives) are used to quickly transfer electrons away from the donor materials. Due to the close energy match between the LUMO levels of donor and acceptor, when an exciton reaches the interface of donor and acceptor, ultra-fast electron transfers can occur (e.g. transfer of a photoinduced electron from the LUMO of the donor to the LUMO of the acceptor, leaving a hole (h^+) in the HOMO of the donor).[9] Ultrafast photophysical studies show that the time required for electron transfer is around 45 fs; this is much faster than the competing electron-hole recombination processes, such as luminescence, where lifetimes around > 1 ns are often observed.[10] After the separation of excitons, the electrons and holes are then transported and collected at the respective electrodes. The difference in the work functions of the electrode materials is the driving force for charges to flow outside of junction, where a low work-function metal is used for the collection of electrons and a high work-function metal is used for the collection of the holes.

To obtain a PV device, the following conditions must be met: (1) the energy of the incident light has to exceed the band gap of the donor material (HOMO-LUMO energy gap of polymer) so that the electrons can be excited to LUMO level; (2) the correct offset of band gaps between the donor and acceptor (as shown in Figure 1.2 (a)) is another requirement for photoinduced electron transfer occur; (3) the photoinduced exciton must reach the interface of the donor and acceptor. Excitons created by the absorption of photons can diffuse over a specific distance, usually around 10-20 nm, before undesired electron-hole recombination occurs. Thus, the separation distances between the donor and acceptor interfaces must be less than the exciton diffusion length, otherwise energy loss

6

via exciton decay either by radiative (such as luminescence) or non-radiative (e.g. thermal emission) pathways will occur, and that portion of potential energy is then lost from power conversion.[11]

1.1.2 Bulk heterojunction solar cells.

The polymeric bulk heterojunction solar cell (BHJSCs) architecture described above is the most successful device arrangement in terms of attaining high PCEs and thus is the most widely studied. A BHJSCs device consists of an active layer sandwiched by two dissimilar electrodes, indium tin oxide (ITO) for collection of the positive charge and a metal with high electrical conductivity (backside contact, usually Al) to collect electrons. The active layer is the heart of the device, and is made of an intimate blend of donor and acceptor materials. Conjugated polymers and high-electron-affinity fullerene derivatives are commonly used as electron donor and acceptor materials, respectively. The major reason why BHJSCs give high device performances is that a well inter-mixed donor and acceptor blend greatly increases the interfacial area (by orders of magnitude) and results in a significant decrease of the phase separation length to 10-20 nm. This length scale is similar to the diffusion length of an exciton in photovoltaic polymers; thus, the excitons can reach the donor-acceptor interface much more easily.[12] Hence, the chances of an exciton undergoing decay or recombination is greatly decreased since approximately for every photoinduced exciton, there is a neighboring interface with acceptor that can be reached where fast electron transfer takes place.

1.1.3 Critical parameters for solar cells

PCEs is the core value used to evaluate the performance of solar cells, and it can be defined by four parameters in following equation:

$$PEC = \frac{V_{OC} \cdot I_{SC} \cdot FF}{P_{in}} \qquad (1)$$

Where V_{oc} is the open circuit voltage, I_{sc} is the short circuit current, FF is the fill factor, and P_{in} is incident light power (which has been standardized at 1000 W/m^2). The theoretical maximum open circuit voltage, V_{oc}, is given by the difference of energy level between HOMO of the donor and the LUMO of the acceptor. As can be seen by Equation 1, higher V_{oc} values lead to an increase in the power that the cell can provide. I_{sc} is the current generated by V_{oc} under a short circuit condition, and a higher I_{sc} value demonstrates the cell can more efficiently convert incident photon to current in a short circuit. The fill factor, FF, is ratio of actual power output over theoretical maximum power output can be described mathematically in the equation below, where V_{op} and I_{op} are voltage and current that can be generated at maximum power.

$$FF = \frac{V_{OP} \cdot I_{OP}}{V_{OC} \cdot I_{sc}} \qquad (2)$$

1.1.4 Current challenges of polymer-based solar cells

Despite the promising features of polymeric BHJSCs, these materials have yet to compete with traditional, dominant Si-based PV materials on the market. There are a few significant drawbacks which keep polymer-based solar cells from being widely

commercialized: (1) their relatively low PCEs (2) current difficulties in synthesis, (3) short device lifetimes.

1.1.4.1 Usual causes of low PCEs in BHJSCs

First and foremost, low PCEs is the primary obstacle that has to be overcome. Even though the reported PCEs has been steadily increasing over the past decade,[13] with the recent highest PCEs for organic solar cells was 9.2 % reported by Mitsubishi Chemicals,[14] this value is still far below the current leading gallium arsenide solar cells with a maximum reported efficiency of 28.2 % for unconcentrated sunlight, and 29.1 % with concentrated sunlight.[15] Moreover, even commercially available crystalline-Si-based solar cells have efficiencies in the range of 12 to 20 %.[16]

Each p-n junction in solar cell has its own Shockley–Queisser limit, which is the major cause of low PCEs. According to studies done by Shockley–Queisser, the maximal PCEs for a single p-n junction is 33.7 %, and the ideal band gap to achieve the maximal PCEs is 1.1 eV (1100 nm).[17] Shockley–Queisser limit is attributed to three physical properties of solar cells. The first is blackbody radiation which states all matter with temperature above 0 K will constantly emit radiation that cannot be captured and leads to a 7% loss of incoming energy in inorganic solar cell devices. The second form of energy loss is recombination of an exciton where electrons and holes are inevitably recombined and give off a photon instead of moving to the respective electrodes of the cell. Theoretical calculations show that recombination further reduces device performance by 10% over total incident energy. The last portion of energy loss is incomplete absorption of solar spectrum. Photons with less energy than the optical band gap of the photovoltaic

material are not able to excite electrons, and these photons interact instead with thermal emission in the form of non-radiative rovibrational pathways. This portion is the most significant source of energy loss and accounts for about a 48% loss in PCEs theoretically. According to theory, the Shockley-Queisser limit which is graphically described in Figure 1.4, the maximum PCEs can be obtained when a single p-n junction with a band gap is approximately 1.1 eV, and for polymer-based BHJSCs, the ideal band gap can be approximately 1.6 eV. Unfortunately, the most of semi-conducting polymers for donor materials have band gaps higher than 2 eV.[7] For example, poly-3-hexylthiophene (P3HT), the most widely used donor material in BHJSCs, only harvests photons with wavelengths below ~650 nm, which is a small portion of solar spectrum.[18]
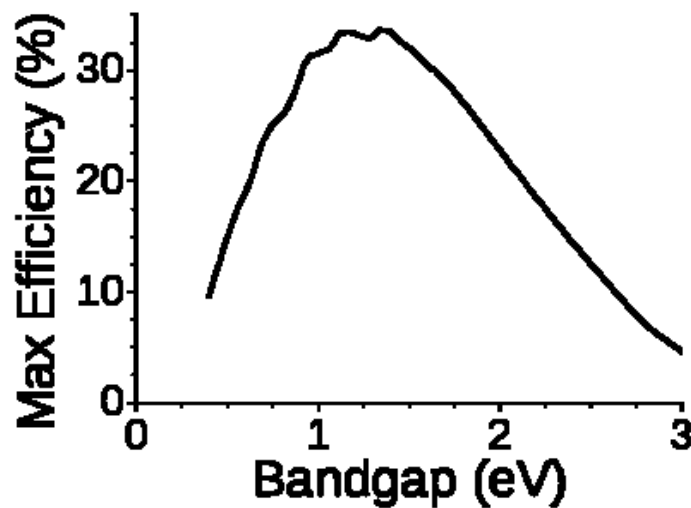
Figure 1.4 The Shockley-Queisser limit for the efficiency of a single p-n junction.

1.1.4.2 Difficulties associated with polymer synthesis and short device lifetimes

The complicated and tedious nature of the synthetic routes used to prepare many photovoltaic polymers, and the short lifetimes of resulting PV devices cannot be ignored as other significant factors that limit the use of PBSCs. As an example, 2,6-bis(trimethyltin)-4,8-dioctylbenzo[1,2-*b*:4,5-*b'*]dithiophene (Figure 1.5), a very common building block used to construct conjugated polymers featuring small band gaps, requires 10 synthetic steps to prepare,[19] which leads to a dramatic increase in fabrication cost. In addition, device lifetimes still remain unsatisfactory. Three major degradation pathways usually exist in PV devices:[20] (1) photo-oxidation of the polymer, resulting in a reduction in conjugation, incident solar photon absorption, and charge-transportation; (2) gradual loss of the conductive properties at the interfaces of the organic device; and (3) mechanical breakdown, such as segregation of the donor and acceptor components in a bulk heterojunction structure over time. Encapsulation technologies can increase device lifetimes by preventing oxidation from occurring; however, it also greatly diminishes the pre-existing advantage of high flexibility within PBSCs and adds considerable manufacture cost.
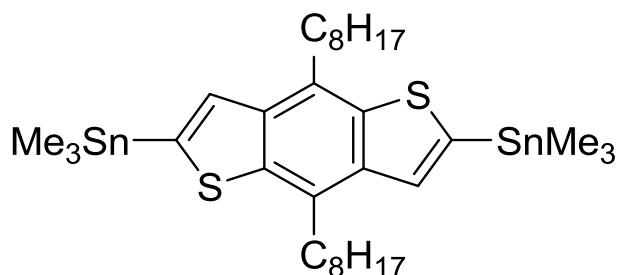
Figure 1.5 Structure of 2,6-bis(trimethyltin)-4,8-dioctylbenzo[1,2-b:4,5-b']dithiophene

1.2 Strategies to improve cell performance

As mentioned, fullerenes are most the commonly used electron acceptor materials for BHJSCs, with solution-processable derivatives, such as [6,6]-phenyl-C_{61}-butyric acid methyl ester ($PC_{61}BM$) or [6,6]-phenyl-C_{71}-butyric acid methyl ester ($PC_{71}BM$) being widely used (Figure 1.6).[21] Relative to polymeric donors, acceptor materials have received less research attention. On the other hand, because the polymeric donor layer is where the harvest of solar energy occurs, active research interests have been given to developing new conjugated polymers with optical band gaps that approach the theoretical optimal values of 1.6 eV. Examples of high performance donor and acceptor materials are shown in Figure 1.5.
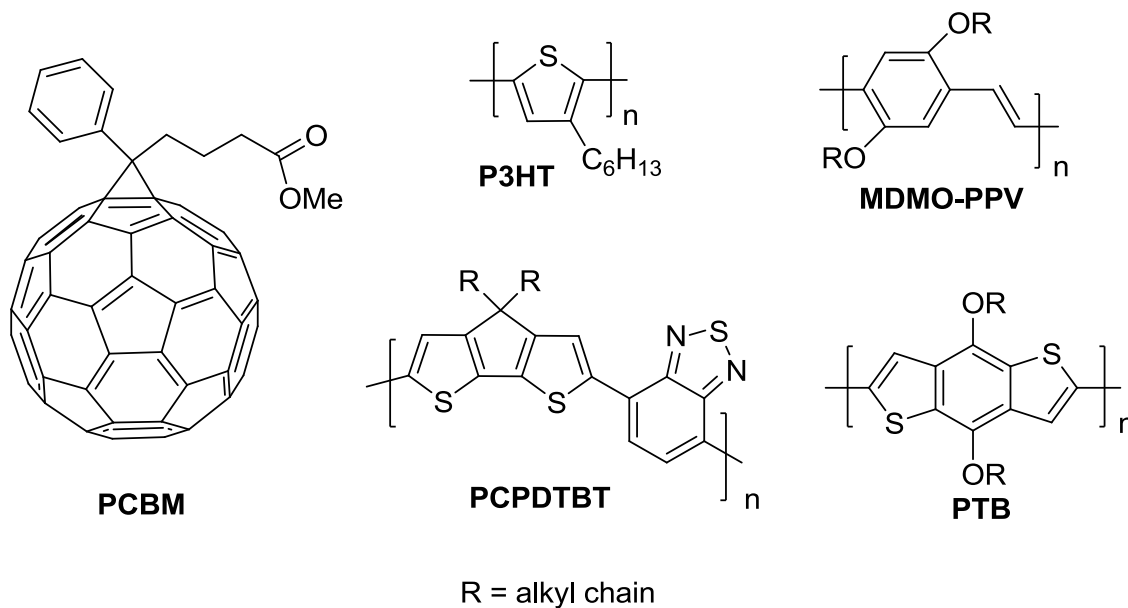
Figure 1.6 Common materials used in PBSCs. PCBM is acceptor material, while the remaining polymers are donor materials.

Tremendous efforts have been devoted towards preparing better materials for PBSCs, and as a result, some general criteria for ideal PV polymers have emerged: (1) the polymer should possess a relatively narrow band gap in order to absorb solar spectrum more thoroughly. (2) The polymer should have moderate solubility in organic solvents for solution processing and printing methods. (3) The HOMO energy level of the polymer should be deep-lying to give a high V_{oc} after blending with PCBM. (4) The energy level offset between polymer (donor) and PCBM (acceptor) should be well-controlled to facilitate the separation of charges while minimizing the energy loss. (5) The polymer should have high hole (h^+) mobility for efficient charge transport.[22]

The common approaches to meet those goals include polymer design,[23] optimizing processing conditions,[24] interface control,[25] and altering morphology of the active layers.[26] Each approach has been actively studied, but tuning of the band gap through polymer design is still the most commonly used approach. Thus extensive research has been devoted towards developing simple synthetic routes for new, stable polymers which can absorb a wider portion of incident solar radiation.[27]

1.3 Advantages of main group heterocycles and their potential use in PV technologies

As seen already, many photovoltaic polymers contain 5-membered heterocycles as part of their chemical structures. Amongst those 5-membered heterocycles, sulfur-containing rings, such as thiophene and its derivatives, are most common. However, the presence of main group element-containing heterocycles other than thiophene in conjugated polymers is still rare, and the synthesis of rings where the sulfur atom is replaced by other inorganic elements (such as Se, Ge, etc) is much less studied. Despite

13

this, the construction of new polymers of varying elemental composition could lead to improve PV performance. For example, polyselenophenes (such as P3HS in Figure 1.7) is expected to have advantages over polythiophenes. Specifically, it has been shown that incorporation of selenophene units into conjugated polymers can reduce the band gap by mainly stabilizing LUMO more efficiently than in corresponding polythiophene analogues. Importantly, the smaller band gap in P3HS was achieved through lowering the LUMO level and not raising HOMO level; thus, the band gap in the donor layer can be lowered without compromising V_{oc} and the overall PCE.[28]
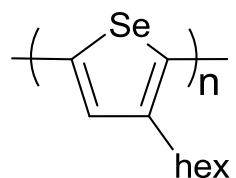
poly(3-hexyl)selenophene (P3HS)

Eg = 1.6 eV
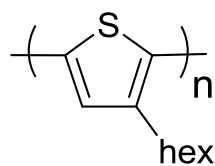
poly(3-hexyl)selenophene (P3HT)

Eg = 1.9 eV

Figure 1.7 Band gap comparisons of **P3HS** and **P3HT**.

Recently, Seferos et al. have conducted a systematic study towards placing sulfur, selenium, and tellurium into copolymers. The absorption spectra of the reported inorganic polymers are shown in Figure 1.8.
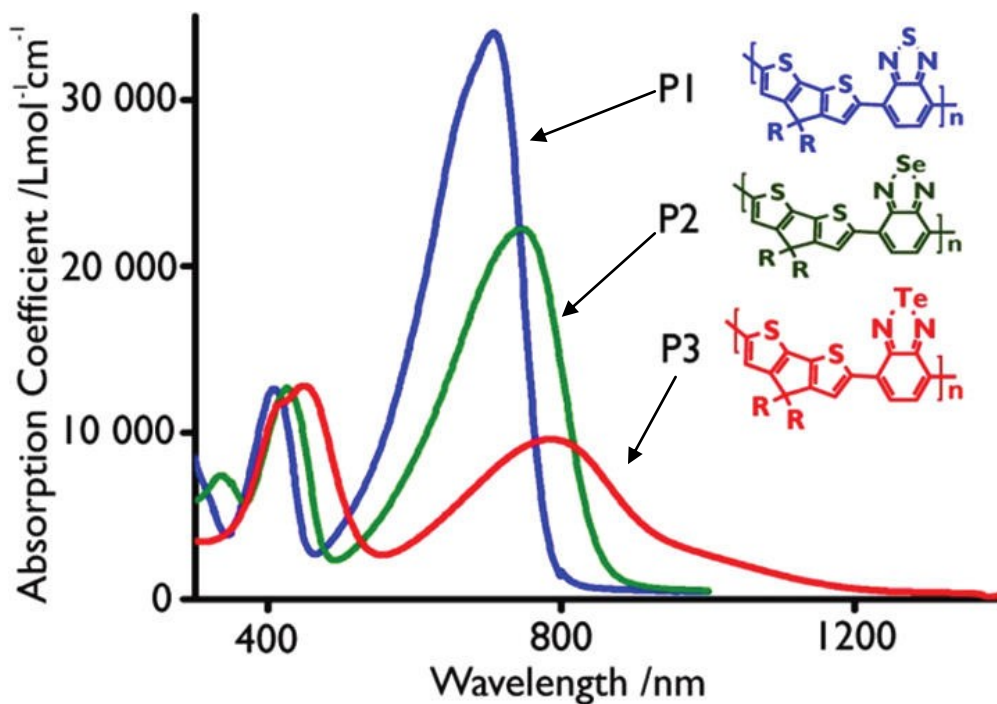
Figure 1.8 Absorption spectra of Group 16-containing copolymers, **P1−P3**.[29]

We can see that the λ_{max} of the three copolymers in Figure 1.8 contain high-energy absorption bands (400 nm ~ 450 nm) which remain relatively unchanged upon moving down the periodic table from S to Se to Te. More remarkably, the λ_{max} of the second low-energy bands, shift significantly from S to Se to Te leading to a narrowing of the optical band gap from 1.59 to 1.46 to 1.06 eV respectively.[29]

Moreover, Reynolds *et al*. have synthesized poly-(dithienogermole) (**Polymer-Ge**) and poly-(dithienosilole) (**Polymer-Si**) polymers (Figure 1.9). **Polymer-Si** and **Polymer-Ge** were blended with the acceptor material PCBM to give active layers for BHJSCs devices. The performances of the devices featuring **Polymer-Si** or **Polymer-Ge** are summarized in Table 1.1.

Polymer-Ge when X= Ge

or

Polymer-Si when X = Si
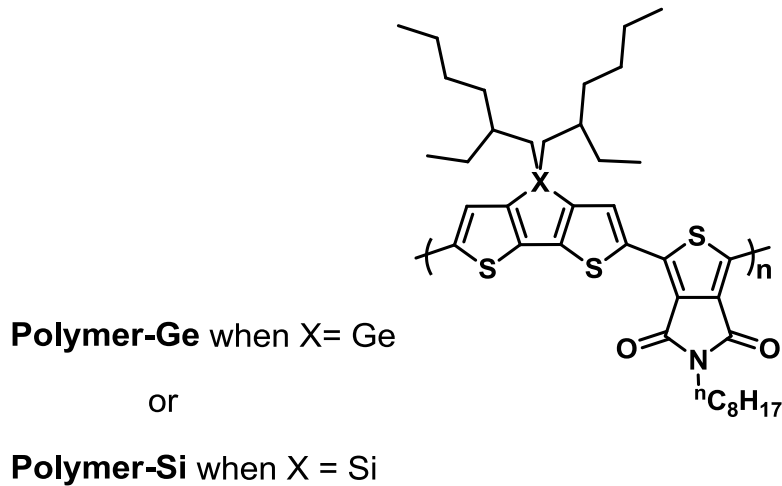
Figure 1.9 Example of a polydithienogermoles and a polydithienosiloles.

Table 1.1: Comparison of device performances featuring **Polymer-Si** and **Polymer-Ge**

	PEC	Fill Factor	$I_{sc}(mA/cm^2)$	V_{oc} (V)	EQE (visible region)
Polymer-Si:PCBM	6.6%	65%	11.5	0.89	50%-56%
Polymer-Ge:PCBM	7.3%	68%	12.6	0.85	55%-65%

We can see that most parameters used to evaluate device performance in Table 1.1 are higher for **Polymer-Ge** except for V_{oc}. The smaller V_{oc} for **Polymer-Ge** is due to the smaller band gap for **Polymer-Ge**, which is achieved through raising HOMO **Polymer-Ge**, leading to a slight reduction in V_{oc}. [30]

Based on the interesting properties of the two examples above, the incorporation of inorganic heterocycles of varying composition is a promising route towards improving BHJSCs device performance. However, one currently existing challenge is the lack of an

efficient route to preparing polymers that contain germole, selenophene, or tellurophene units.

Seferos *et al*. in 2010 reported the first successful synthesis of a well-defined stable polytellurophene (Figure 1.10) via palladium-catalyzed polycondensation chemistry;[31] a major challenge is this route is the need to begin with the parent tellurophene which is prepared in very low yield (Scheme 1.1 (a)).[32]
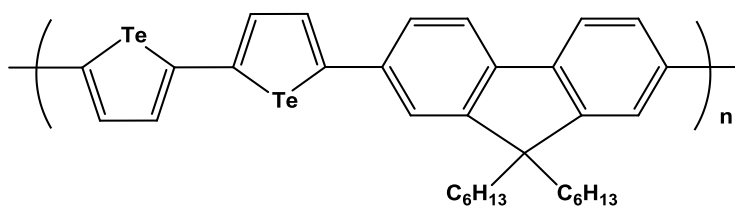
Figure 1.10 Tellurophene-containing copolymer

Similarly, the synthesis of polyselenophene often involves multiple steps and requires challenging synthetic procedures to prepare the required starting material, selenophene (Scheme 1.1(b)).[33] The challenges associated with the syntheses of these inorganic heterocycles is an important reason why the study of these novel conjugated units has been quite limited. Therefore, it would be of significant benefit if we can find an easier procedure to prepare these heterocycyles.

(a)

(b)
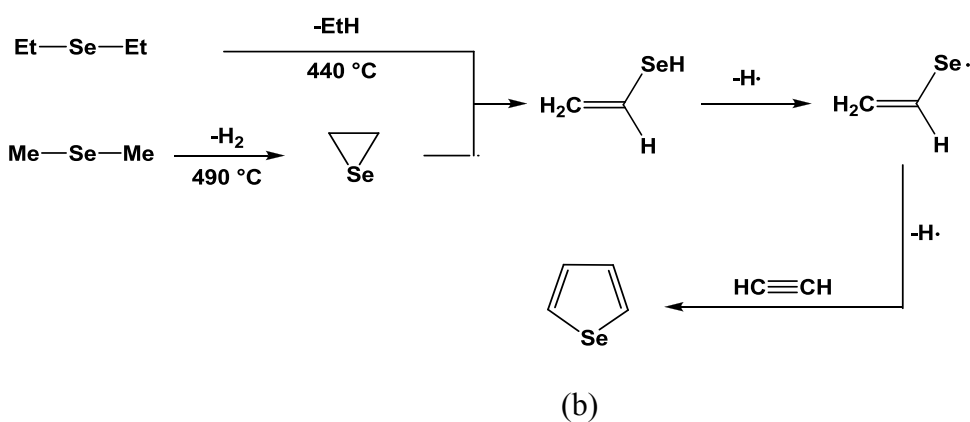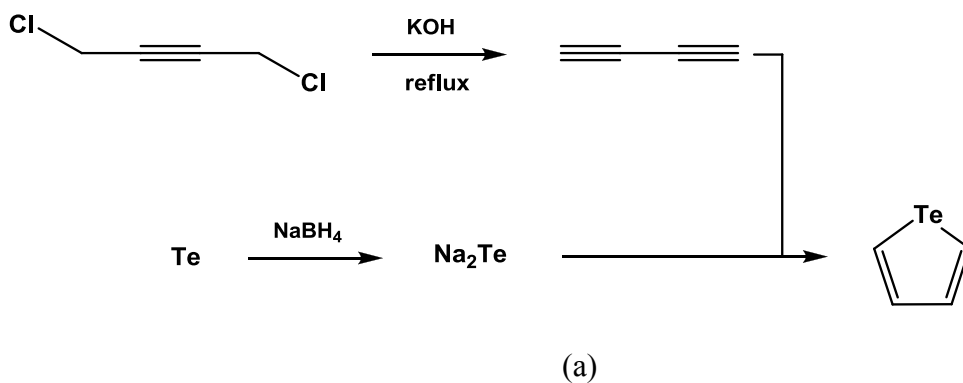
Scheme 1. 1 Synthesis of (a) tellurophene and (b) selenophene

1.3.1 Insights from zirconium-mediated metallacycle transfer and its application to the synthesis of conjugated heterocycles

In 1988, Fagan *et al.* discovered a synthetic route which provides easy access to various heterocyclic compounds via metallacycle transfer of a readily available zirconacyclopentadiene[34,35] (Scheme 1.2). There are a number of advantages associated with the synthesis of main group heteroles by metallacycle transfer chemistry. These include: (1) facile access of main group heteroles where conventional syntheses are laborious, tedious, and fraught with safety issues; (2) selective control over the nature of

the inorganic elements incorporated into the conjugated system; (3) the most remarkable

feature of the metallacycle transfer reaction is its generality, which allows us prepare

heteroles derivatives containing almost every p-block main group element.
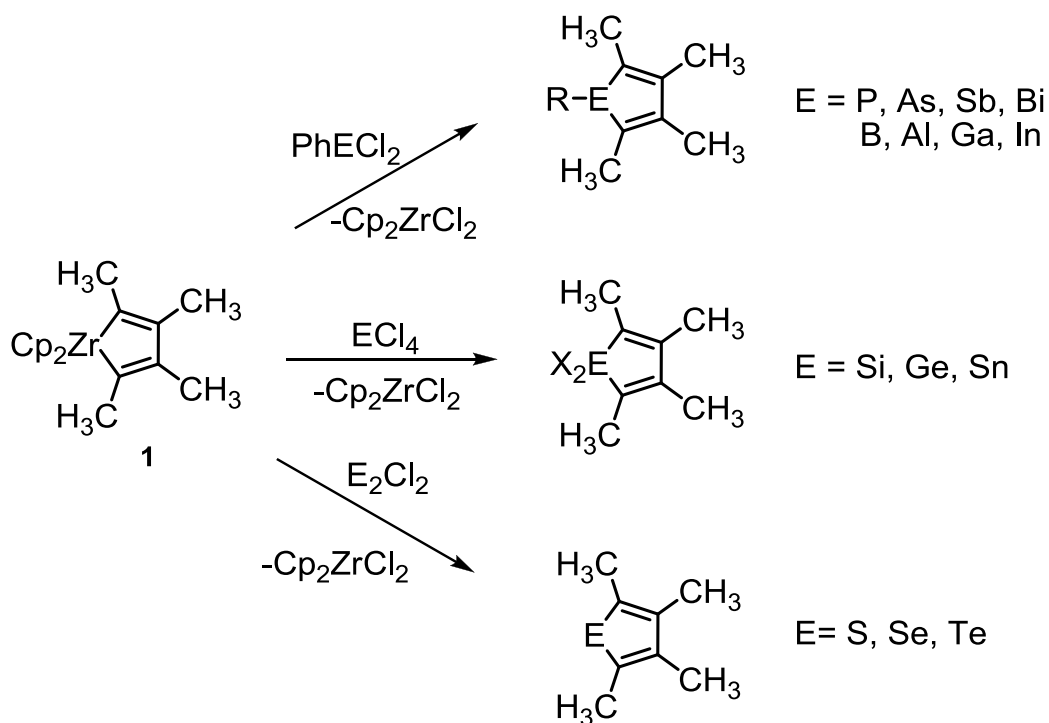
Scheme 1. 2 Examples of metallacycle transfer starting from the zirconacyclopentadiene precursor **1**.

Since changing the nature of the main group heterocycles in conjugated polymers

has been shown to be an effective way of controlling the electronic and optical properties

of the resulting material, metallacycle transfer chemistry can be a useful method to affect

the electronic and optical properties of polymers by incorporating different main group

elements. This Thesis will focus on the use of metallacycle transfer chemistry as a means

of accessing new photovoltaic polymers featuring tunable band gaps. However, before

this method can be used to synthesize conjugated polymers, there are two reactions that need to be conducted: (1) the synthesis of a zirconacycle as a precursor for metallacycle transfer; (2) the incorporation of zirconacycles into a conjugated polymeric systems or as a part of polymerizable monomers.

1.3.2 Synthesis of zirconacycles and metallacycle transfer chemistry

Zirconacycles are essential precursors that must be prepared before metallacycle transfer chemistry can occur (Scheme 1.2). The formation of a zirconacyclopentadiene requires reductive coupling of alkynes by a zirconocene unit, "Cp_2Zr". Even though there are several methods to generate sources of "Cp_2Zr", the most common procedure is the one developed by Negishi *et al*. (Scheme 1.3). The procedure is still widely used due to its synthetic convenience and high yield, and this method involves treatment of Cp_2ZrCl_2 with 2 equivalents of ^nBuLi for 1 h at -78°C in THF; the in situ generated "Cp_2Zr" is then reacted with alkynes to form zirconacyclopentadienes (Scheme 1.3).[36]
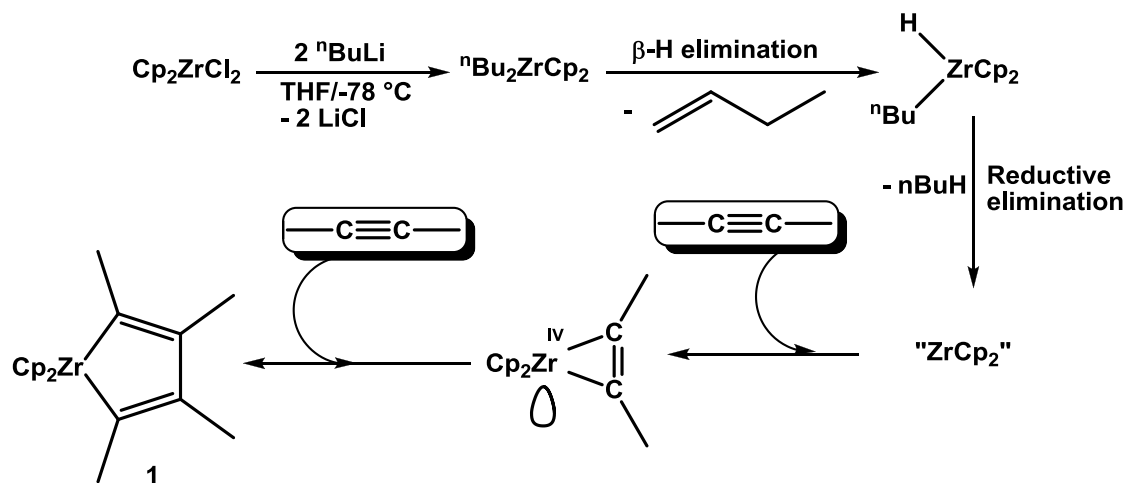
Scheme 1.3 Synthesis of the Nigeshi reagent "Cp_2Zr" and formation of zirconacyclopentadienes from alkyne coupling.[37]

Scheme 1.3 illustrates an example of zirconacyclopentadiene formation via zirconocene coupling of 3-butyne. The initial reaction between Cp_2ZrCl_2 and ^nBuLi in THF is first yields dibutylzirconocene, which is thermally unstable and undergoes β-H elimination. The formation of "Cp_2Zr" was studied in depth by Harrod *et al.*[38], and his studied revealed that β-H elimination from a butyl group was a dominant process (Scheme 1.3), and that many other intermediates (> 12) were also present in solution. This reaction mixture, termed "Cp_2Zr", reacts as a 14-electron Zr^{II} species, and is capable of interacting with many unsaturated alkynes to give zirconacyclopentadienes.

The zirconacyclopentadienes generated via alkyne coupling can then readily undergo metallacycle transfer chemistry. The nature of the main group halide has a profound influence on the success of the metallacycle transfer reaction. For example, when $SiCl_4$ is combined with zirconacyclopentadienes virtually no reactivity is observed; however, $GeCl_4$ rapidly reacts in high yield to give a germole (and Cp_2ZrCl_2 as byproduct). Fagan *et al.* have noted that the metallacycle transfer will proceed smoothly with main group halides that possess a coordination sphere can be readily expanded and highly polar E—X bonds.[35]

A possible mechanism for the zirconium-mediated metallacycle transfer reaction is given in Figure 1.11. In each step, there is a four-centered transition state involved (σ bond metathesis), wherein a Zr—C bond is cleaved to form a new E—C bond along with halide transfer to Zr (Figure 1.11). Meanwhile, it has been noticed that substitution of halides (X) with alkyl chains (typically methyl or ethyl) can greatly slow down the rate of transfer (*e.g.* $SnCl_4$ reacts much faster than Me_2SnCl_2). A detailed study of the

mechanism of metallacycle transfer should gives us a better understanding about what elements we should choose and what substituents should be attached for the future synthesis of conjugated polymers in an efficient manner.

R= alkyl chain

X = halides
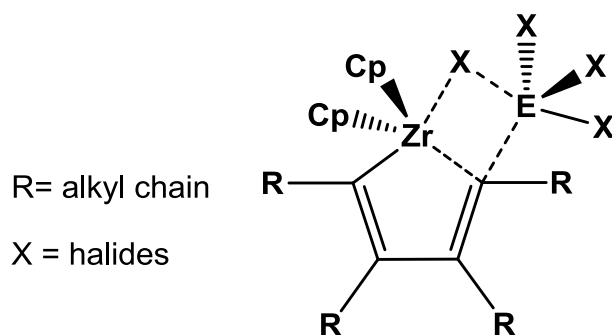
Figure 1.11 Transition state of metallacycle transfer.

1.4 Incorporation of zirconacyclopentadienes into a polymer

The heterocycle, tetramethylzirconacyclopentadiene (**1**), discussed in the previous section cannot be directly polymerized. In order to incorporate different main group elements into conjugated polymer, we have to either insert zirconacyclopentadiene units into the main chain of a polymer (followed by metallacycle transfer chemistry) or synthesize a monomer which can be polymerized after metallacycle transfer. Those two ideas will be illustrated in detail in subsequent sections.

1.4.1 Zirconocene coupling with aryl-spaced diynes

Nishihara *et al*. started exploring an organometallic approach to the synthesis of conjugated polymers. The synthetic method involved the reaction of a cobalt complex, CpCo(PPh$_3$)$_2$, with 4,4-diethynylbiphenyl to form a conjugated polymer containing alternating cobaltacyclopentadiene and biphenyl units.[39]

Tilley *et al.* merged this concept with zirconocene coupling and made a series of important contributions towards the synthesis of zirconacycle-containing polymers over the past two decades. In 1995, Tilley *et al.* reported the synthesis of the zirconium-containing polymer **3** by the direct zirconocene coupling of a diyne **2** with an aryl group spacer (Scheme 1.4).[40] However, studies of this silylene/zirconacyclopentadiene polymer were only limited to its hydrolysis to form **4** and related iodinolysis chemistry; meanwhile, the authors did not perform metallacycle transfer chemistry with this polymer.
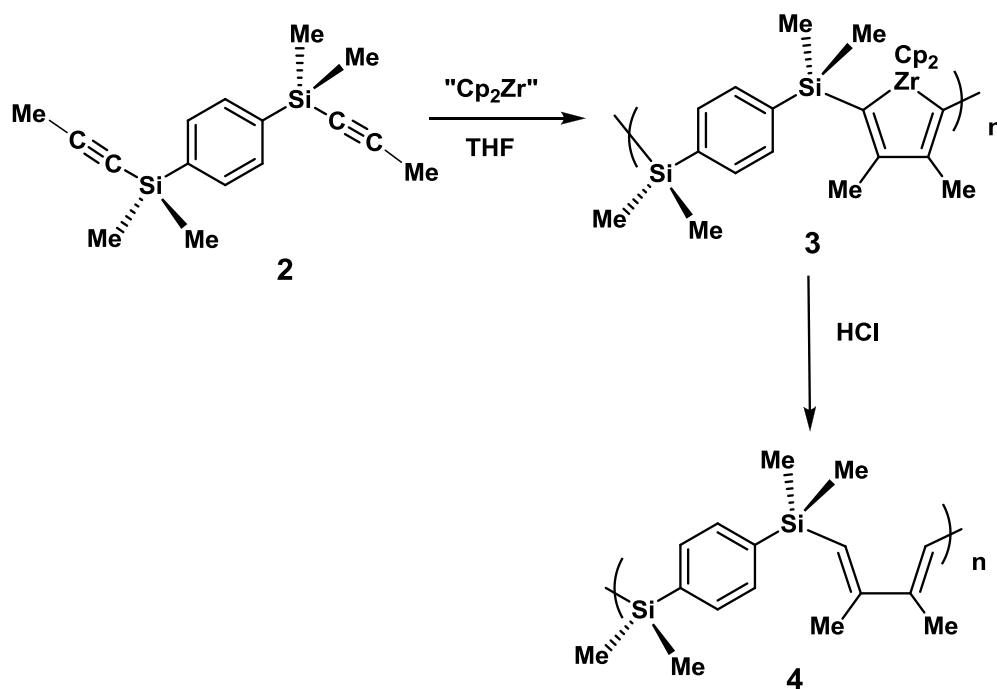
Scheme 1. 4 Synthesis of the zirconacycle-containing polymer **3** and the hydrolyzed polymer **4**

In 1997, Tilley *et al*. first reported the synthesis of a conjugated inorganic polymer based on the use of the zirconocene coupling with diynes followed by metallacycle transfer. [41] Condensation of the diyne ($^{n}C_5H_{11}$)C≡CC$_6$H$_4$C$_6$H$_4$C≡C($^{n}C_5H_{11}$) (**5**) with Negishi's reagent "Cp$_2$Zr" afforded the zirconacycle-containing polymer **6** (Scheme 1.5). The presence of pentyl groups in the polymer promoted its solubility in common organic solvents, while the diphenyl spacer units served to enhance the conjugation along the main chain. The authors further explored metallacycle transfer with **6** to give polymers containing phosphole and thiophene rings (**7** and **8**, respectively). However, there was an inherent flaw in this synthetic route. The zirconacyclopentadiene-containing polymer **6** possessed a structure consisting of both 2,4 and 2,5 connected metallacycle units in the polymer backbone in a ratio of 4:1 (see Scheme 1.5); the result showed that zirconocene coupling with asymmetric diynes was not regioselective, which matched observations made previously. [42] Importantly, even though electronic properties can be tuned by chemical modification of alkyne starting materials, the lack of a regular structure lead to polymers (**7** and **8**) that had wider than anticipated band gaps (Table 1.2), which limited their potential use in solar cell technologies.
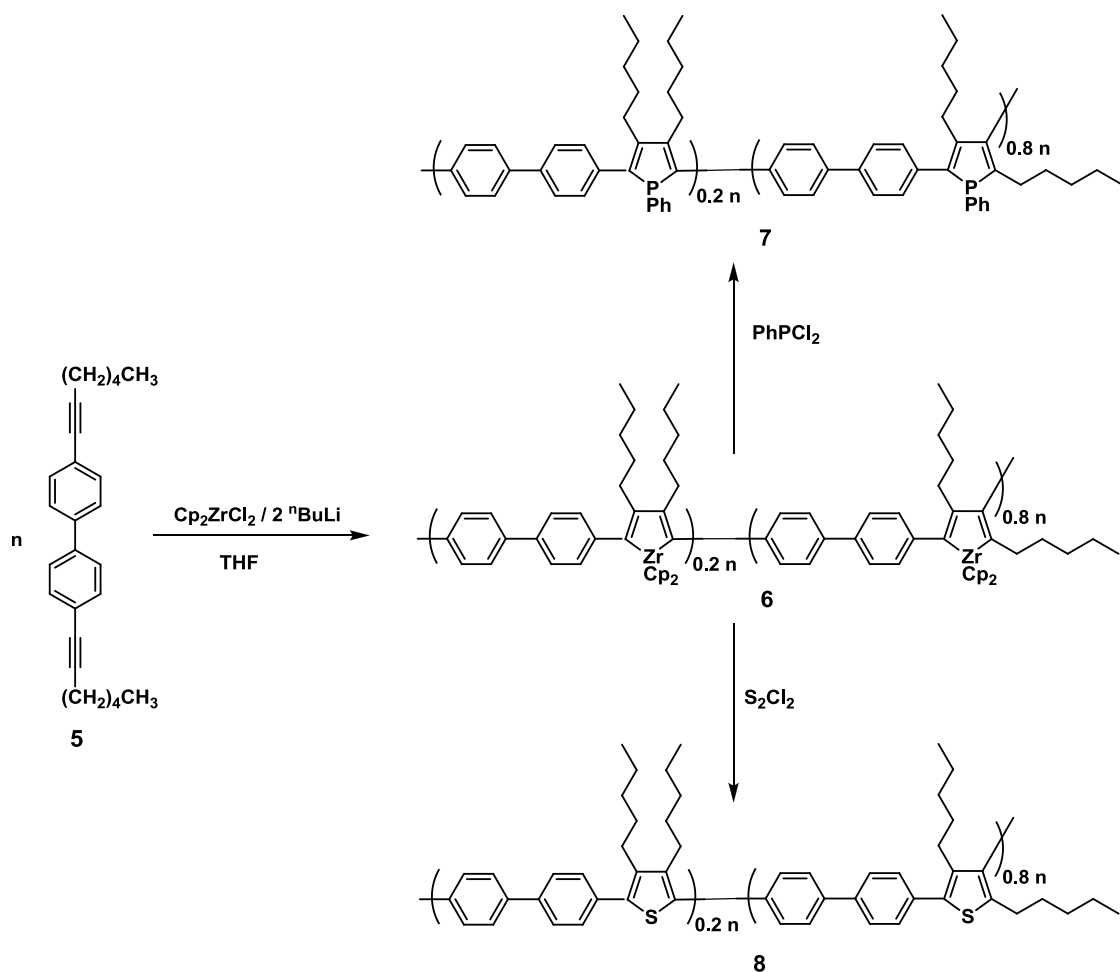
Scheme 1.5 Synthesis of polymer **6** and performance of metallacycle transfer chemistry to give polymers **7** and **8**

Table 1.2 Absorption and emission properties of polymers **6**, **7**, and **8**

Polymers	λ_{max} (nm)	λ_{em} (nm)
6	296	398
7	308	470
8	316	426

1.4.2 Using zirconocene coupling with alkyl-chain-spaced diynes

In 1998, Tilley and coworkers further improved upon the synthetic route introduced in Scheme 1.5 to yield polymers with regioregular structures (Scheme 1.6). This approach takes advantage of regioselective, ring-closing coupling of diynes that are linked by flexible alkyl spacer groups (Equation 3).[43]
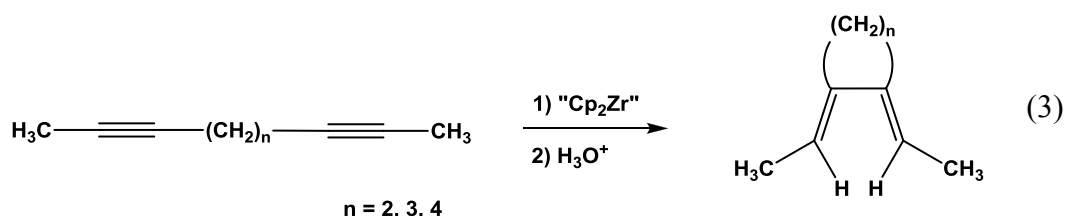
The improved synthesis first started with the preparation of a poly(arylenediyne) (**9**) via palladium-catalyzed cross-coupling followed by intramolecular zirconocene coupling and hydrolysis to form poly(arylenedieneylene)s (Scheme 1.6). Variation of the substituents on the aryl group and changing the size of the alkyl rings on the diene allowed for tuning of the optical absorption and emission energies of the polymers.[44] It was found that absorption and emission spectra were red-shifted as the alkyl ring size was decreased. We can see that the product of zirconocene coupling with the polymer diyne **9** afford only one regioisomer **10** based on this synthetic route; however, the approaches the author used to tune the optical properties was through altering substituents and backbone structure (R and x in Scheme 1.6) instead of performing metallacycle transfer chemistry with the zirconacyclopentadiene units.
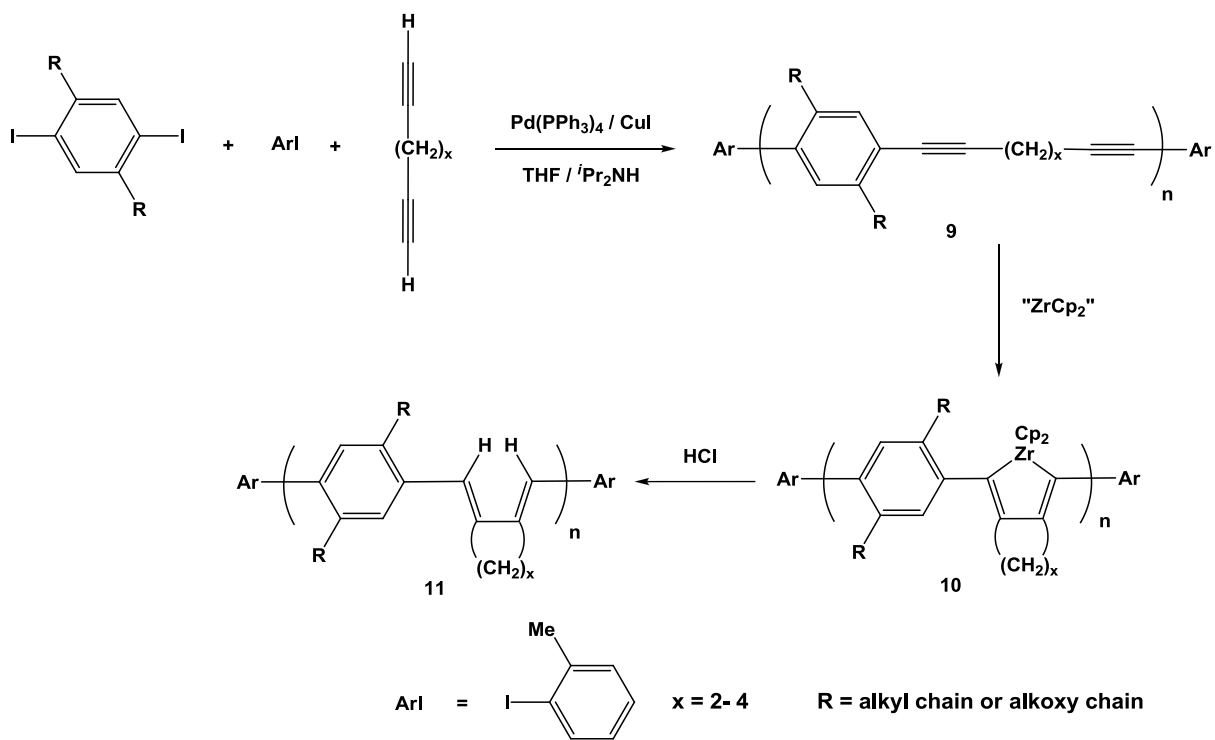
Scheme 1. 6 Synthesis of conjugated polymers via zirconocene coupling with alkyl-spaced diynes.

1.5 Two possible strategies towards the syntheses of conjugated polymers via metallacycle transfer that will be explored in this Thesis.

After reviewing Tilley's excellent work, some potential areas of improvement in the synthetic routes described in Scheme 1.5 and 1.6 was noted: instead of using phenyl and biphenyl groups as building blocks in the conjugated polymers, we would like to incorporate thiophene rings into the main chain as thiophene rings have already been shown to yield materials with better electronic and optical properties for photovoltaic applications (*e.g.* P3HT).

The scope of the metallacycle transfer reaction was not fully explored by the groups of Tilley and Fagan. In terms of obtaining polymers, only preliminary trials involving the synthesis of P and S-containing polymers were reported in Scheme 1.5, and the synthetic routes used did not give polymers with regioregular structures. The synthetic route in Scheme 1.6 did afford zirconacyclopentadienes with regioregular structures; unfortunately, metallacycle transfer chemistry was not performed in this study. Thus, we will try to take full advantage of the generality of metallacycle transfer chemistry. We wish to incorporate rings containing heavy main group elements into polymers in order to tune the band gap for potential use in BHJSCs.

Polymer defects also affect the purity and the extent of conjugation in the final polymers. After analyzing Tilley's synthetic routes for preparing conjugated polymers in Scheme 1.5 and 1.6, we found that the preparation of conjugated polymers via multiple steps requires chemical conversion of one polymer structure to another using zirconocene coupling, metallacycle transfer, or hydrolysis. Incomplete conversion in each step is unavoidable and can undoubtedly result in unreacted defect sites in the polymers. Tilley *et al*. also admit that the clean conversion of Zr polymers to new conjugated polymers may not be quantitative. Taking the above factors into consideration, we focused on two strategies in order to prepare new conjugated polymers featuring tunable band gaps.

1.5.1 Strategy one: synthesis of conjugated polymers via zirconocene coupling with thiophene-spaced bis-alkynes

We acknowledge that using zirconocene coupling with bis-alkynes is a promising route to directly incorporate zirconacyclopentadiene units into a main chain of a polymer;

moreover, the presence of alkyl side chains can promote solubility of the polymers. As mentioned in the previous section, we will use thiophene groups as a conjugated building block. Starting from the thiophene-based diynes (**12**), we hope to prepare the alternating thiophene/zirconacyclopentadiene copolymers (**13**). In a final step, we seek to prepare a series of main group element-containing (such as Sn, Ge, Se, etc) conjugated polymers via metallacycle transfer chemistry (Scheme 1.7).
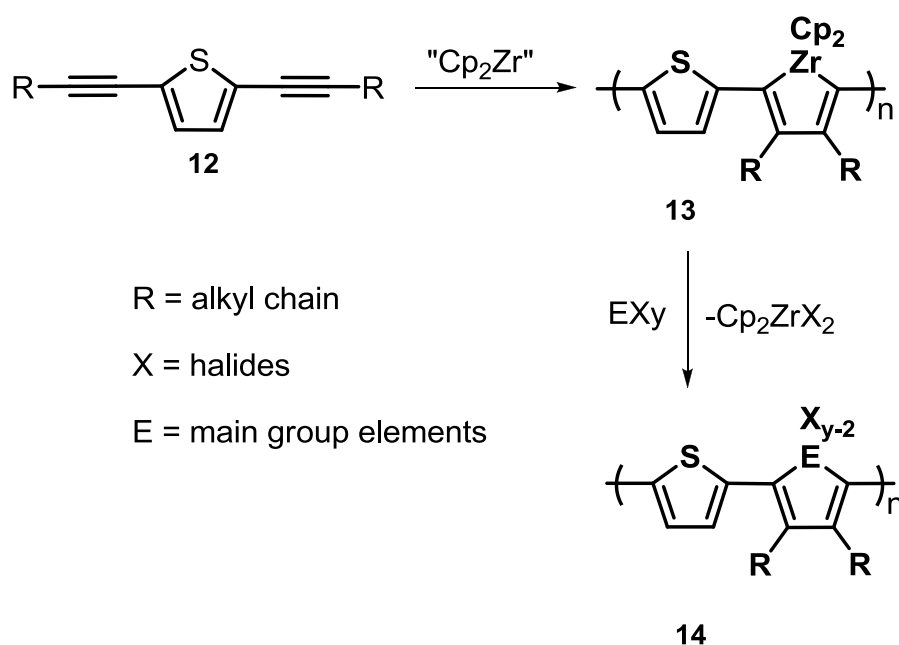
Scheme 1. 7 The synthetic route for Strategy one to give main group element-containing polymers (**14**).

1.5.2 Strategy two: synthesis of conjugated polymers via monomeric zirconacycles

It is possible that the zirconium-containing polymer in Strategy one may suffer from irregular and cross-conjugated structures (similar to in Scheme 1.5) due to non-

regioselective zirconocene coupling with the asymmetric alkyne; therefore, it might be a challenge to obtain polymers in pure form using the first strategy (Section 1.5.1). Even if the synthetic route shown in Scheme 1.7 can give regioregular polymers, incomplete substitution of Cp_2Zr in the polymer by main group elements possess another hurdle.

Consequently, in order to prepare conjugated polymers with regioregular structures and to minimize the chance of defects in the polymer, the synthetic method illustrated in Scheme 1.6 will be modified (Scheme 1.8). We will still take advantage of selective coupling of the alkyl-spaced diynes with zirconocene, but will focus on the preparation of monomeric precursors. We will prepare the required thiophene-bromide-capped diynes via well-known Pd(0) catalyzed cross-coupling chemistry. These aryl-group-capped diynes, when coupled with zirconocene, will yield zirconacyclopentadienes **15** in a monomeric form (Scheme 1.8). After performing metallacycle transfer, we hope to obtain a series of conjugated monomers **16** consisting of the desired main group heteroles. Due to the nature of the thiophene-bromide end groups in the monomers, we should be able to further polymerize the pure monomers to give high molecular weight polymers for use as photovoltaic materials in BHJSCs.

E = main group elements

Ar =

X = halides

x = 2, 3, 4
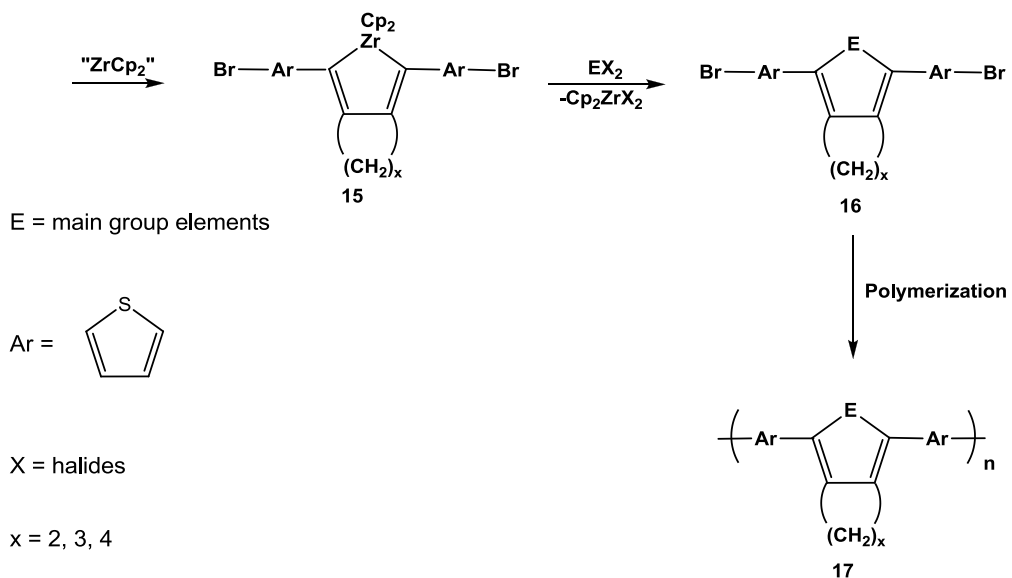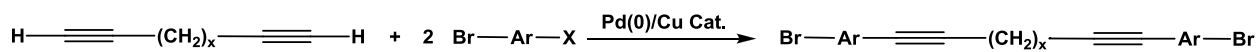
Scheme 1. 8 The synthetic route for Strategy two: Synthesis of conjugated monomers and their polymerization.

1.6 References

[1] More than 100 countries from Solarbuzz, "Solarbuzz Report World Solar Photovoltaic Market Grow to 18.2 Gigawatts in 2010, Up 139% Y/Y," Solarbuzz.com, 15 March 2011.

[2] Geotzberger, A.; Hebling, C.; Schok, H.-W. "Photovoltaic Materials, History, Status, and Outlook," *Mater. Sci. Eng.* R, vol. 40, pp. 53-94, **2003**.

[3] Gennler, G.; Sariciftci, N. S. *Proceedings of the IEE*, **2005**, *93*, 1492.

[4] (a) Shaheen, S. E.; Radspinner, R.; Peyghambarian, N.; Jabbour, G. E. *Appl. Phys. Lett.* **2001**, *79*, 2996. (b) Sirringhaus, H.; Kwase, T.; Friend, R. H.; Shimoda, T.; Inbasekaran, M. *Science* **2000**, *290*, 2123.

[5] Gunes, S.; Neugebauer, H.; Sariciftci, N. S. *Chem. Rev.* **2007**, *107*, 1324.

[6] Chaing, C. K.; Fincher, C. R.; Park, Y. W.; Heeger, A. J.; Shirakawa, H.; Louis, E. J.; Gua, S. C.; MacDiarmid, A. G. *Phys. Rev. Lett.* **1997**, *39*, 1098.

[7] Tang, C. W. *Appl. Phys. Lett.* **1986**, *48*, 183.

[8] Nunzi, J. M. *C. Rev. Physique* **2002**, *3*, 523.

[9] Sariciftci, N. S.; Smilowitz, L.; Heeger, A. J.; Wudl, F. *Synth. Met.* **1993**, *59*, 333.

[10] Mozer, A.; Zerza, G.; Cerullo, G.; De Silvestri, S.; Luzatti, S.; Hummelen, J. C.; Sariciftci, N. S. *Chem. Phys. Lett.* **2001**, *340*, 232.

[11] Mozer, A.; Sariciftci, N. S. *R. Chimie* **2006**, *9*, 568.

[12] Hoppe, H.; Sariciftci, N. S. *J. Mater. Chem.* **2004**, *19*, 1924.

[13] (a) Peet, J.; Kim, J. Y.; Coates, N. E.; Ma, W. L.; Moses, D.; Heeger, A. J.; Bazan, G. C. *Nat. Mater.* **2007**, *6*, 497. (b) Kim, Y.; Cook, S.; Tuladhar, S.; Choulis, S. A.; Nelson, J.; Durrant, R. J.; Bradley, D. C.; Giles, M.; McCulloch, I.; Ha, C.-S.; Ree, M. *Nat. Mater.* **2006**, *5*, 197. (c) Blouin, N.; Michaud, A.; Gendron, D.; Wakim, S.; Blair, E.; Neagu-Plesu, R.; Belletete, M.; Durocher, G.; Tao, Y.; Leclerc, M. *J. Am. Chem. Soc.* **2008**, *130*, 732.

[14] Service, R. F. *Science* **2011**, *332*, 293.

[15] (a) Single junction thin-film record PCEs (unconcentrated sunlight): http://spectrum.ieee.org/green-tech/solar/solar-cell-breaks-efficiency-record, accessed on Feb 2012. (b) Single junction thin-film record PCEs (concentrated sunlight): M. A. Green, K. Emery, Y. Hishikawa, W. Warta, E. D. Dunlop. *Prog. Photovolt: Res. Appl.* **2011**, *19*, 565.

[16] Jager-Waldau, A. *PV Status Report 2012*, **2012**, *European Commission*, EUR 24807 EN.

[17] Shockley, W.; Queisser, H. J. *J. Appl. Phys.* **1961**, *32*, 510.

[18] Brabec, C. J. *Sol. Energy Mater. Sol. Cells* **2004**, *83*, 273.

[19] Liang, Y.; Feng, D.; Wu, Y.; Tsai, S.; Li, G.; Ray, C.; Yu, L. *J. Am. Chem. Soc.* **2009**, *131*, 7792.

[20] Deibel, C.; Dyakonov, V. *Rep. Prog. Phy.* **2010**, *73*, 096401.

[21] Haufler, R. E.; Conceicao, J.; Chibante, L. F. P.; Chai, Y.; Byrne, N. E.; Flanagan, S.; Haley, M. M.; O'Brien, S. C.; Pan, C.; Xiao, Z.; Billups, W. E.; Ciufolini, M. A.;

Hauge, R. H.; Margrave, J. L.; Wilson, L. J.; Curl, R. F.; Smalley. R. E. *J. Phys. Chem.* **1990**, *94*, 8634.

[22] Chu, T.-Y.; Lu, J.; Beaupre, S.; Zhang, Y.; Pouliot, J.-R.; Wakim, S.; Zhou, J.; Leclerc, M.; Ding, J.; Tao, Y. *J. Am. Chem. Soc.* **2011**, *133*, 4250.

[23] (a) Zou, Y.; Najari, A.; Berrouard, P.; Beaupre, S.; Reda, B.; Tao, Y.; Leclerc, M. *J. Am. Chem. Soc.* **2010**, *132*, 5330. (b) Hou, J.; Chen, H.-Y.; Zhang, S.; Chen, R. I.; Yang, Y.; Wu, Y.; Li, G. *J. Am. Chem. Soc.* **2009**, *131*, 15586. (c) Tsai, J.-H.; Lee, W.-Y.; Chen, W.-C.; Yu, C.-Y.; Hwang, G.-W.; Ting, C. *Chem. Mater.* **2010**, *22*, 3290. (d) Wang, E.; Ma, Z.; Zhang, Z.; Vandewal, K.; Henriksson, P.; Zhang, F.; Anderson, M. R. *J. Am. Chem. Soc.* **2011**, *133*, 14244.

[24] (a) Jo, J.; Kim, S.-S.; Na, S.-I.; Yu, B.-K.; Kim, D.-Y. *Adv. Funct. Mater.* **2009**, *19*, 866. (b) Peet, J; Kim, J. Y.; Ma, W. L.; Moses, D.; Heeger, A. J.; Bazan, G. C. *Nat. Mater.* **2007**, *6*, 497. (c) Li, G.; Chu, C.-W.; Shrotriya, V.; Huang, J.; Yang, Y. *Appl. Phys. Lett.* **2006**, *88*, 253503.

[25] (a) Stein, R.; Kogler, F. R.; Brabec, C. J. *J. Mater. Chem.* **2010**, *20*, 2499. (b) Sharma, G. D.; Suresh, P.; Sharma, S. S.; Vijay, Y. K.; Mikroyannidis, J. A. *Appl. Mater. Interfaces* **2010**, *2*, 504. (c) Khlyabich, P. P.; Burkhart, B.; Thompson, C. B. *J. Am. Chem. Soc.* **2011**, *133*, 14534.

[26] (a) Yodyingyong, S.; Zhou, X.; Zhang, Q.; Triampo, D.; Xi, J.; Park, K.; Limketkai, B.; Cao, G. *J. Phys. Chem.* **2010**, *114*, 21851. (b) Tung, C. V.; Kim, J.; Cote, J. L.; Huang, J. *J. Am. Chem. Soc.* **2011**, *133*, 2962. (c) Coffin, R. C.; Peet, J.; Rogers, J.; Bazan, G. C. *Nat. Chem.* **2009,** *1*, 657.

[27] (a) Huo, J; Chen, H.-J.; Zhang, S.; Chen, R. I.; Yang, Y.; Wu, Y.; Li, G. *J. Am. Chem. Soc.* **2009**, *131*, 1558. (b) Perzon, E.; Zhang, F.; Anderson, M. R.; Mammo, W.; Inganas, O. *Adv. Mater.* **2007**, *19*, 3308. (c) Welch, G. C.; Coffin, R.; Peet, J.; Bazan, G. C. *J. Am. Chem. Soc.* **2009**, *131*, 10802. (d) Lee, S. K.; Lee, W.-H.; Cho, J. M.; Park, J. S.; Park, J.-U.; Shin, W. S.; Lee, J.-C. Kang, I.-N.; Moon, S.-J. *Macromolecules*, **2011**, *44*, 5994. (e) Wang, M.; Hu, X.; Liu, P.; Li, W.; Gong, X.; Huang, F.; Cao, Y. *J. Am. Chem. Soc.* **2011**, *133*, 9638.

[28] Heeney, M.; Zhang, W.; Crouch, D. J.; Chabinyc, M. L.; Gordeyev, S.; Hamilton, R.; Higgins, S. J.; McCulloch, I.; Skabara, P. J.; Sparrowe, D.; Tierney, S. *Chem. Commun.* **2007**, *43*, 5061.

[29] Gibson, G. L.; McCormick, T. M.; Seferos, D. S. *J. Am. Chem. Soc.* **2011**, *134*, 539.

[30] Amb, C. M.; Chen, S.; Graham, K. R.; Subbiah, J.; Small, C. E.; So, F.; Reynolds, J. R. *J. Am. Chem. Soc.* **2011**, *133*, 10062.

[31] Jahnke, A. A.; Howe, G. W.; Seferos, D. S. *Angaw. Chem. Int. Ed.* **2010**, *49*, 10140.

[32] Sweat P. D.; Stephens, E. C. *J. Organomet. Chem.* **2008**, *693*, 2463.

[33] Deryagina, E. N.; Sukhomazova, E. N.; Levanova, E. P.; Korchevin, N. A.; Danilova, A. P. Russ. *J. Org. Chem.* **2004**, *40*, 290.

[34] Fagan, P. J.; Nugent, W. A. *J. Am. Chem. Soc.* **1988**, *110*, 2310.

[35] Fagan, P. J.; Nugent, W. A.; Calabrese, J. C. *J. Am. Chem. Soc.* **1994**, *116*, 1880.

[36] Negishi, E.; Cederbaum, F. E.; Takahashi, T. *Tetrahedron Lett.* **1986**, *27*, 2829.

[37] Negishi, E.; Takahashi, T. *Bull. Chem. Soc. Jpn.* **1998**, *71*, 755.

[38] Dioumaev, K. V.; Harrod, F. J. *Organometallics*, **1997**, *16*, 1452.

[39] Ohkubo, A.; Aramaki, K.; Nishihara, H. *Chem. Lett.* **1993**, *22*, 271.

[40] Mao, S. S. H.; Tilley, T. D. *J. Am. Chem. Soc.* **1995**, *117*, 5365.

[41] Mao, S. S. H.; Tilley, T. D. *Macromolecules*, **1997**, *30*, 5566.

[42] Takahashi, S.; Kuroyama, Y.; Sonogashira, K.; Hagihara, N. A. *Synthesis*, **1980**, 627.

[43] Nugent, W. A.; Torn, D. L.; Harlow, R. L. *J. Am. Chem. Soc.* **1987**, *109*, 2788.

[44] Lucht, L. B.; Mao, S. S. H.; Tilley, T. D. *J. Am. Chem. Soc.* **1998**, *120*, 4354.

Chapter 2: Synthesis of Conjugated Polymers via Zirconium-mediated Metallacycle Transfer Chemistry

2.1 Introduction

Conjugated polymers have been intensely studied by the scientific community as photovoltaic and light emitting materials due to their unique features such as being flexible, lightweight, and inexpensive to produce. [1] Bulk heterojunction solar cells (BHJSC), which consist of electron donor and acceptor materials, are the most successful polymer-based solar cell device structure so far, wherein conjugated polymers act as electron donor photovoltaic materials. However, due to incomplete absorption of solar irradiation, the resulting low power conversion efficiencies (PCEs) of BHJSC have significantly limited their use in energy generation applications. The presence of high optical band gaps within many conjugated polymers is a major factor that causes lower PCEs; therefore, an important research theme during the past decade involves lowering the band gap of conjugated polymers to an optimal value, 1.6 eV. [2]

In order to tune optical band gaps and achieve high PCEs, researches have focused on changing the polymer composition, the processing conditions[3] and tuning the interface morphology[4] of the active layers in BHJSC devices. Among those efforts, band gap manipulation via the synthesis of new conjugated polymers is widely acknowledged as a one of the most effective approaches to improving PCEs; thus, it is an active field of study. As shown by previous studies, polymers bearing five-membered heterocycles such as polythiophene (and their derivatives) have desirable photovoltaic properties which allows for their use as building units in electron donor materials in BHJSC devices. On the other hand, polymers containing main group heterocycles other than sulfur in the

main chain are still rare, and incorporating main group heteroles into conjugated polymers is a research method towards achieving improved polymer solar cell device performance.

Recent studies have shown that polymers having main group elements, such as selenium or phosphorus, can offer attractive electronic and optical properties. For instance, polyselenophene or alternate copolymers of thiophene/selenophene are expected to have improved photovoltaic properties in solar cells devices according to studies conducted by Zade and Tierney, which showed that selenophene-containing polymers have lower band gaps and deeper LUMO levels than conventional polythiophene-based polymers.[5] Moreover, phosphorus-based polymers containing conjugated phosphole rings are also valuable building blocks for the preparation of conjugated low band gap materials when oligothiophenes are present. In addition, the optical and electronic properties of these polymers can be further tuned by chemical modification of the P-atom of the phosphole rings.[6] Therefore it is worthy to further understand how the presence of other main group elements within conjugated polymers can influence the opticoelectronic properties.

Fagan *et al*. have demonstrated that metallacycle transfer chemistry of zirconacyclopentadienes with a variety of main group elements halides yields a wide range of heterocycles featuring group 13-16 elements (Scheme 2.1).[7]
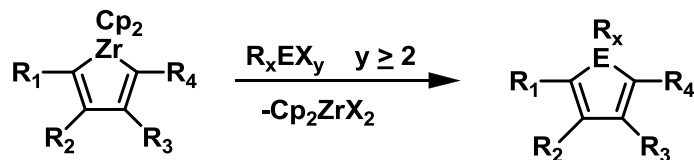
X = halide,

E = group 13-16 element

R = alkyl chain

Scheme 2.1 General description of metallacycle transfer from zirconacyclopentadienes.

If we can incorporate zirconacyclopentadienes into a polymeric system and then perform metallacycle transfer, we will have a potential way to readily prepare a family of conjugated polymers containing different main group elements with potentially useful photovoltaic properties. Notably, the synthesis of polymers containing zirconacyclopentadiene units can be readily achieved by coupling aryl-centered bis-alkynes together using the well-known, in situ generated, Negishi reagent "Cp$_2$Zr". The entire process is depicted in below.
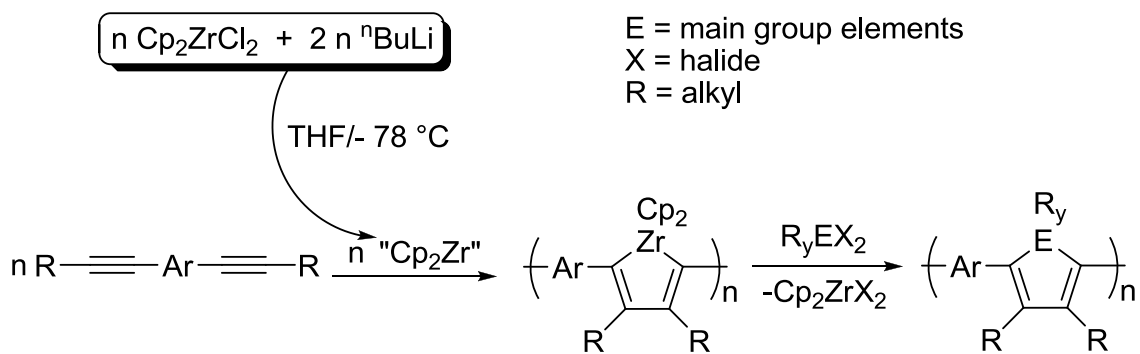
Scheme 2.2 Synthetic route towards conjugated polymers containing main group elements.

Tilley *et al*. have initially explored the approach outlined in Scheme 2.2 for the synthesis of conjugated polymers. The first step of the synthesis was the zirconocene coupling of aryl-linked diynes with in situ produced Cp_2Zr, followed by reaction of resulting the Zr-polymers with main group halides (in a one-pot procedure) to give polymers based on P and S.[8] Given the versatility of metallacycle transfer chemistry involving molecular zirconacyclopentadienes, we hoped to incorporate new element types into conjugated polymers, especially heavy main group elements, and study the optical and electronic properties of the resulting polymers in the context of polymer solar cell applications.

Another route to conjugated polymers would be to start with monomeric zirconacyclopentadienes and then prepare main group elements monomers via metallacycle transfer (Scheme 2.3). In a final step, new polymers can be obtained through the polymerization of those main group monomers. Since several metallacycle transfer reactions will be performed, isolation of the zirconacyclopentadiene precursor will bring convenience to our studies as we can examine a series of diffferent metallacycle transfer reactions at one time by simply mixing zirconacyclopentadiene with desired main group compounds of varying composition. In addition, we think that the synthesis of a polymer from main group monomers can lead to a polymer of higher purity compared to those made using the synthetic route in Scheme 2.2 because we avoid metallacycle transfer chemistry involving a polymer (which has been shown to be problematic in the past).
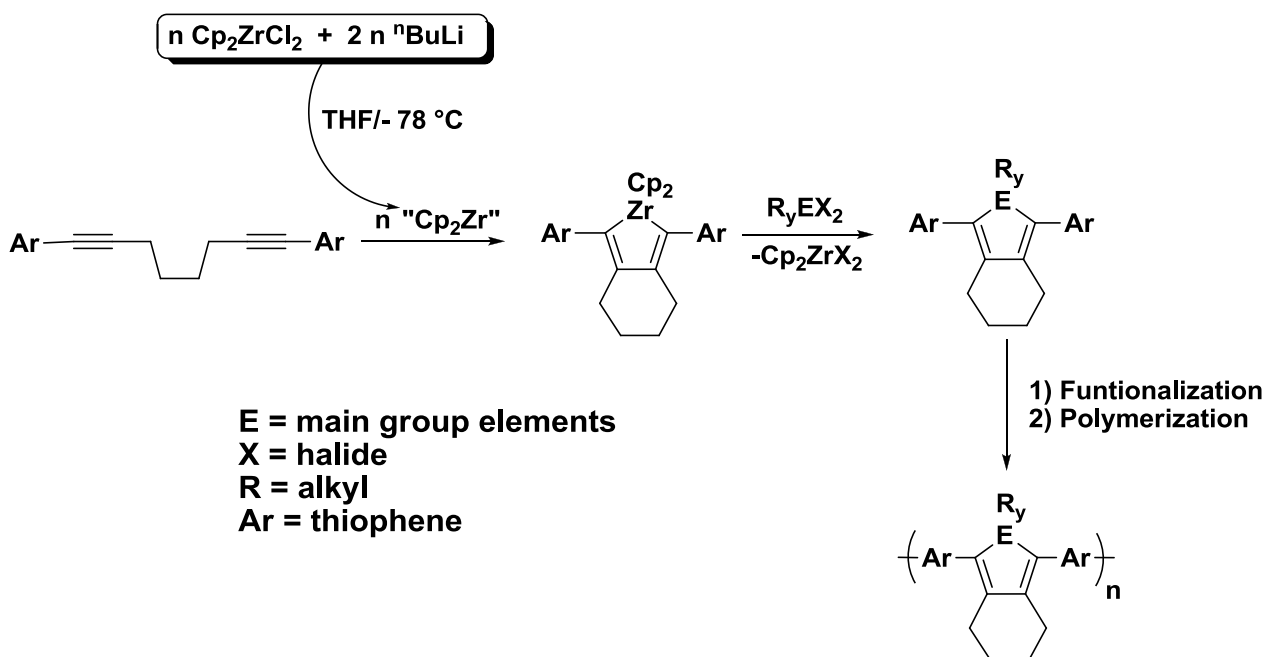
Scheme 2.3 Synthesis of conjugated polymers from monomeric zirconacyclopentadienes.

In this chapter, we investigate the use of metallacycle transfer to prepare a series of monomers and polymers containing heavy main group elements. This work highlights the potential of metallacycle transfer chemistry as a synthetic route to quickly obtain a variety of conjugated polymers featuring potential tunable band gaps.

2.2 Results and Discussion

2.2.1 Synthesis of a polymeric zirconacyclopentadiene from an aryl-linked bis-alkyne

Initial attempts to prepare conjugated polymers involved the direct formation of a zirconacycle-containing polymer with thiophene units. The requisite bis(alkyne) **1** was first prepared by the Pd(0)/CuI catalyzed Sonogashira coupling of 1-hexyne with 2,5-dibromothiophene following a known procedure (Scheme 2.5). In a second step, compound **1** was reacted with in situ generated zirconocene, "Cp$_2$Zr" (which was formed

by adding two equiv. of ^nBuLi to a THF solution of Cp_2ZrCl_2 at -78 °C). One possible

mechanism for the formation of "Cp_2Zr" is described in Scheme 2.4.
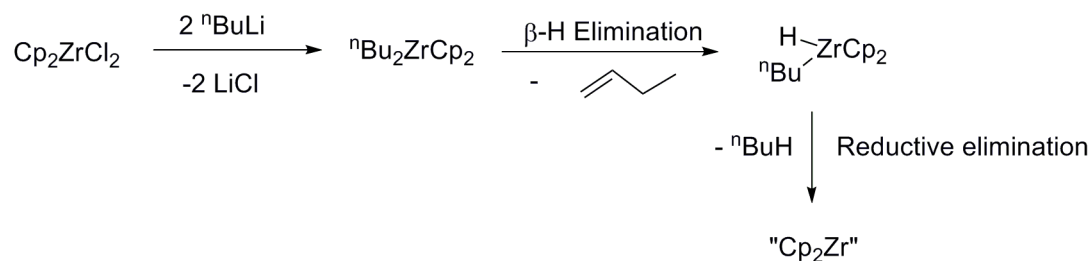
Scheme 2.4 One possible mechanism for the formation of Negishi's reagent "Cp_2Zr".

The resulting air-sensitive polymer **PM1** contained zirconacyclopentadiene units in

the main chain with butyl groups attached onto the Zr-ring (Scheme 2.5). The purpose of

the butyl groups in **PM1** was to improve the solubility of any polymers derived from

PM1, and to encourage the planar orientation of conjugated rings in the polymer in the

solid state leading to lower optical band gaps.
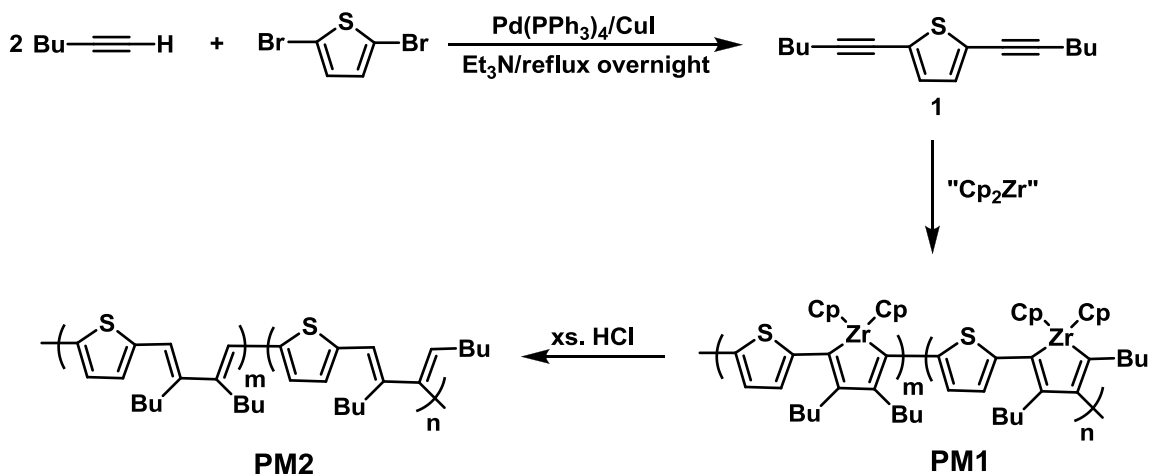
Scheme 2.5 Synthesis of the polymeric zirconacyclopentadiene **PM1** and its hydrolysis.

Importantly, Tilley *et al.* found that the formation of polymers via the zirconium-mediated coupling of diynes was sensitive to reaction conditions and noted the following conditions were necessary to achieve high molecular weight polymers:[9] (1) the amount of ^{n}BuLi used to generate "Cp$_2$Zr" had to be close to 1.95 equivalents per molecule of Cp$_2$ZrCl$_2$, (2) the reaction between Cp$_2$ZrCl$_2$ and ^{n}BuLi in THF had to proceed for 30 min at -78 °C prior to the addition of alkyne **1**; (3) reaction between "Cp$_2$Zr" and the alkyne could not be too long as complicated mixtures were obtained if the reaction was left to proceed for > 8 h.

By taking these above mentioned factors into consideration, a solution of **1** in THF was then added dropwise into a premixed ^{n}BuLi/Cp$_2$ZrCl$_2$ mixture in THF at -78 °C, and then warmed up to room temperature followed by stirring for 4 h. The zirconacycle-containing polymer (**PM1**) was obtained as a deep-red, air- and moisture-sensitive solid. The air-sensitive nature of **PM1** prevented direct molecular weight determination by gel permeation chromatography (GPC); however, the same polymer can be generated in situ using the protocol detailed above and hydrolyzed by carefully adding aqueous HCl. The resulting zirconium-free polymer, **PM2**, was air-stable and dissolved readily in THF; GPC measurement revealed the presence of a high molecular weight material ($M_w = 136$ 000; PDI = 1.35). PM1 and PM2 were then analyzed by NMR spectroscopy, and we noticed that the polymer end groups were not observed, likely due to the high molecular weight of the material.

However, the actual structure of **PM1** and **PM2** was more complicated than originally anticipated. On the basis of the ^{1}H NMR spectrum of **PM1**, there are two broad

singlet resonances due to Cp groups appearing at 6.14 and 6.08 ppm, corresponding to the presence of two distinct Cp_2Zr environments in the polymer. These results are in accord with a previous study done by Tilley,[10] who showed that when the Negishi reagent, "Cp_2Zr", was used to couple unsymmetrical alkynes, $R_1C\equiv CR_2$, three possible products can be obtained (Scheme 2.6). The regiochemistry for the alkyne coupling with "Cp_2Zr" is affected by both steric and electronic factors.[11] For example, the presence of bulky or electron withdrawing groups, such as perfluoroaryl, encourage the formation of zirconacycles with the substituents at the 3,4-positions. However, when sterically unhindered alkyl groups are present on the diynes (such as **1**), the coupling with "Cp_2Zr" is not regioselective and two isomers was observed experimentally (3,4 and 3,5 isomers).[12] Because small alkyl group tend to adopt 3,4 and 3, 5 positions and we observed two "Cp_2Zr" environments in **PM1**, it was concluded that **PM1** had butyl groups at both 3,4 and 3,5-positions and thus the polymer was not regioregular.
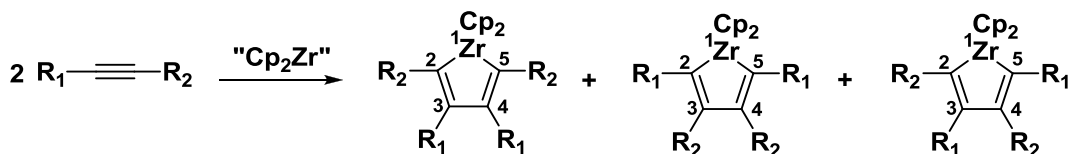
Scheme 2.6 Formation of isomeric products due to zirconocene coupling with unsymmetrical alkynes.

The regioregularity of a polymeric chain can play a key role in determining the optical and conjugation properties of the materials. For example, both optical and charge transport properties of poly-3-hexylthiophene films are known to improve with the degree of regioregularity,[13] and Tilley *et al.* also demonstrated that conjugated polymers

with irregular or cross-conjugated structures possess relatively wide band gaps.[9] Therefore, the regioregularity is an important factor that we have to take into consideration when designing polymers for photovoltaic applications. Meanwhile, there is an additional complication associated with the strategy described in Scheme 2.5. Despite the high yields often obtained in metallacycle transfer chemistry involving molecular zirconacyclopentadienes (~90%), it is likely that a small, yet variable, amount of zirconacycle units will still be inevitably present in main polymer chain after metallacycle transfer chemistry is conducted. Therefore, it will be difficult to control the purity of the resulting inorganic polymers generated by the reaction sequence in Scheme 2.5.

2.2.2 Synthesis of regioregular zirconacycles

In order to circumvent the non-regioselectivity issue, the diyne **1** used in Scheme 2.5 was modified. Instead of using a rigid thiophene spacer unit within the diyne, zirconocene coupling was explored using a diyne in which the alkyne groups were separated by a flexible alkyl linker. This approach allows ring-closing to occur via intramolecular alkyne coupling to give a regioregular material that could be polymerized in a later step. Our initial work involved the synthesis of a zirconacycle model containing two thiophene units at each end of a zirconium heterocycle. The required precursor 1,8-di(thiophen-2-yl)octa-1,7-diyne (**2**) was prepared via a known Sonogashira coupling procedure, involving 1,7-octadiyne and 2-bromothiophene (see Scheme 2.7). The resulting thiophene-substituted diyne was then reacted with in situ generated "Cp$_2$Zr" to form the zirconacycle (**3**) in high yield. Compound **3** has been used previously as an

intermediate for metallacycle transfer,[14] but this zirconacycle was never isolated prior to our study. ^1H and $^{13}C\{^1H\}$ NMR spectroscopy provided evidence for the clean formation of **3**. For example, the Cp groups appeared as a singlet resonance at 6.23 ppm in ^1H NMR spectrum; meanwhile, three spectroscopically shifted thiophene-bound hydrogen atoms were observed, and each appeared as a doublet of a doublets. Two upfield triplet resonances at 2.46 and 1.57 ppm were also detected and were assigned to the CH_2 groups within the six-numbered ring that is fused with the zirconacyclopentadiene unit.
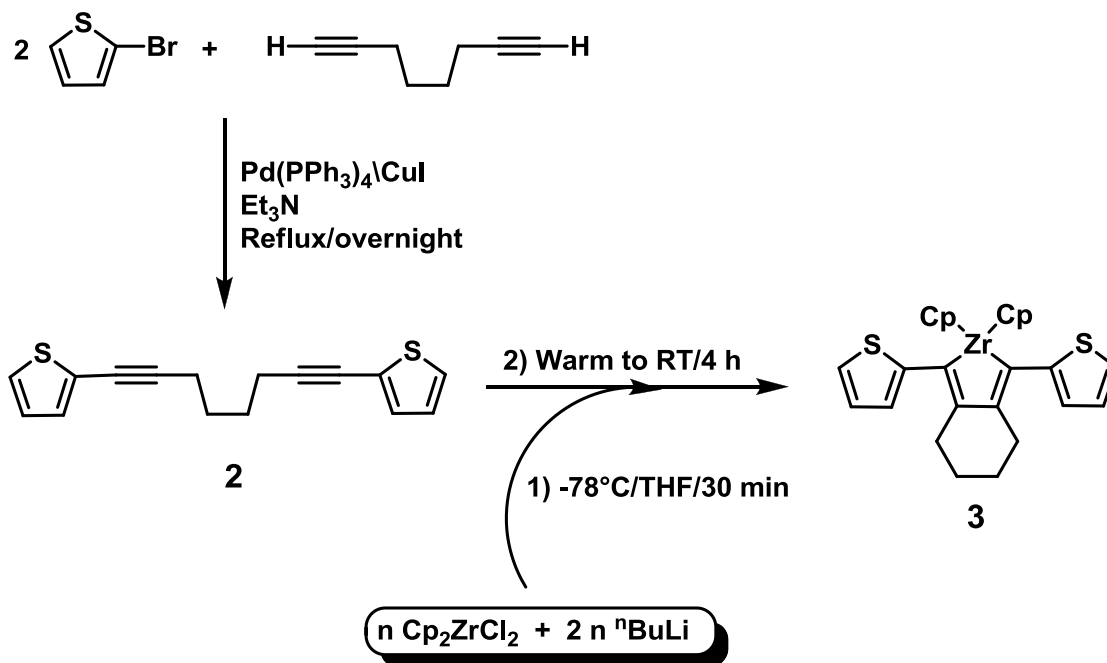
Scheme 2.7 Synthesis of the thiophene-capped zirconacycle **3**.
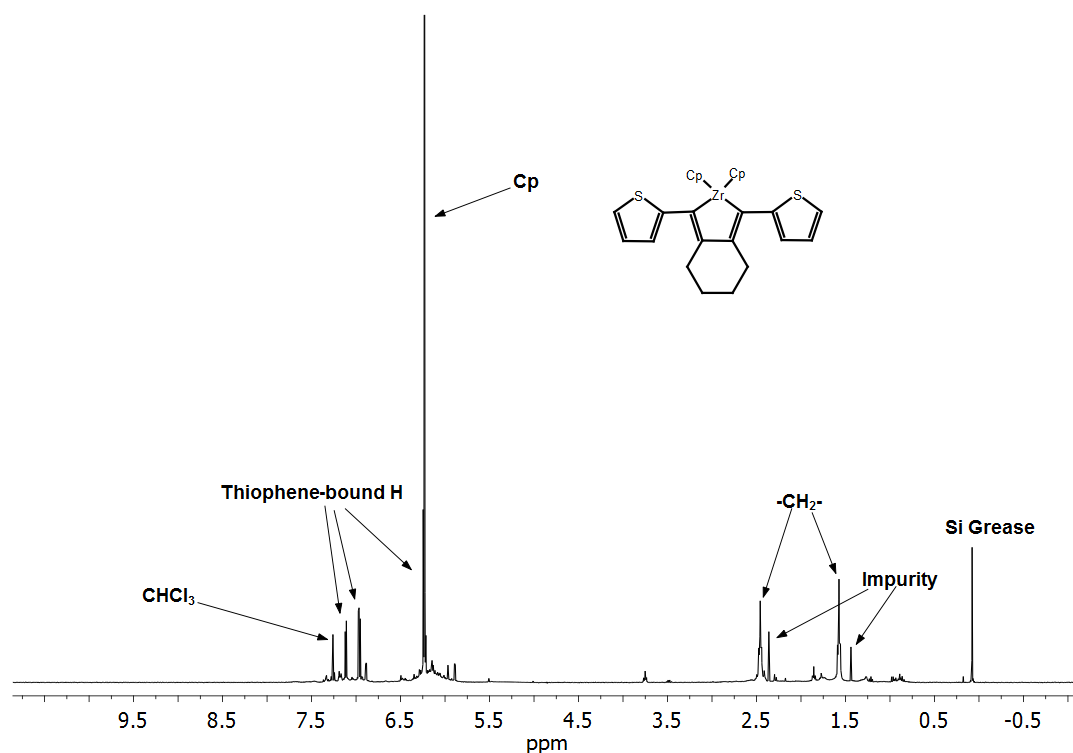
Figure 2.1 ^{1}H NMR spectrum of the zirconacycle **3**.

^{13}C{^{1}H} NMR spectroscopy gave further support for the formation of **3**. A distinct resonance due to the Cp groups was located at 112 ppm and six resonances from 177 to 121 ppm due to aromatic carbon atoms were observed as well. Based on the information obtained from NMR spectroscopy, a single isomer was obtained, and thus this zirconacycle synthesis can be potentially used to form regioregular polymers.

However, presumably, the main group element containing monomers obtained from **3** after metallacycle transfer may not be able to undergo polymerization due to the absence of functional groups on the thiophene rings that can undergo C—C bond forming chemistry to form polymers. Therefore, it was necessary to functionalize the starting

diynes so that various polymerization strategies could be explored at a later stage. Scheme 2.8 outlines our synthesis of the modified zirconacycle **5** that contains reactive bromothiophene end groups. In order to incorporate a bromothiophene unit in a diyne (to form **4**), 2-bromo-5-iodothiophene was reacted with 1,7-octadiyne. Notably the C—I bond in 2-bromo-5-iodothiophene is more vulnerable to undergo Pd-catalyzed cross-coupling so that the Sonogashira coupling reaction in Scheme 2.8 will occur preferentially with iodine leaving the C—Br bond intact. To achieve selective coupling, the reaction was carried out under a mild condition (50 °C) and longer reaction time (48 h). As mentioned, polymerization of a future monomer generated from this bromine-terminated diyne is foreseeable.
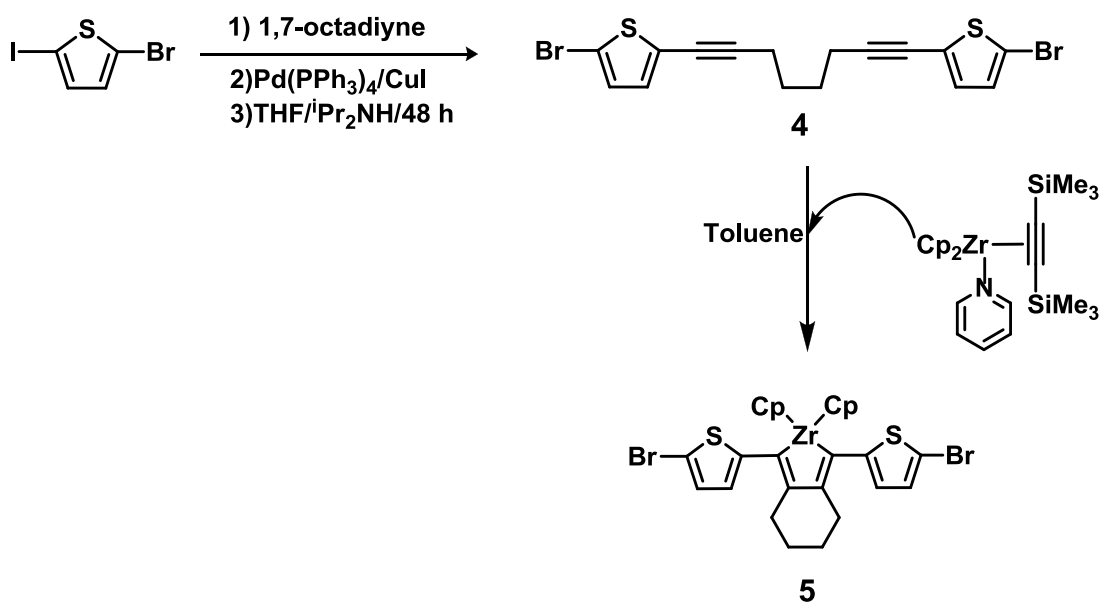
Scheme 2.8 Synthesis of the bromine-terminated zirconacyclopentadiene **5**.

On the other hand, reaction of the diyne **4** with the Negishi's reagent, "Cp$_2$Zr", generated in situ from Cp$_2$ZrCl$_2$ and ^{n}BuLi, can be complicated due to potential Li/Br

48

transmetallation chemistry involving the C—Br bonds in **4** and ^{n}BuLi. Therefore, we chose to use Rosenthal's zirconocene reagent, Cp$_2$Zr(pyridine)(Me$_3$SiC≡CSiMe$_3$), as it can be isolated as a pure, thermally stable, purple solid; thus, it is much easier to control the reagent stoichiometry in alkyne-coupling chemistry.[15]

Gratifyingly, Cp$_2$Zr(pyridine)(Me$_3$SiC≡CSiMe$_3$) reacted cleanly with **4** to give the target zirconacycle **5** as an air- and moisture-sensitive red solid in a high isolated yield of (81%). ^{1}H and ^{13}C{^{1}H} NMR spectra were consistent with expected structure. Unfortunately, compound **5** was only sparingly soluble in common solvents except in THF; thus, we were concerned about the solubility of the resulting materials after metallacycle transfer and polymerization. In order to test the solubility of the monomer yielded from metallacycle transfer, a trial reaction was performed (Scheme 2.9). The reaction between the zirconacycle **5** and SnCl$_4$ gave the intended Sn product **6**. Compound **6** was obtained as a red solid which still contained the byproduct Cp$_2$ZrCl$_2$ after work-up. Both **6** and Cp$_2$ZrCl$_2$ appear to have the same low solubility in organic solvents; thus, it was difficult to separate the **6** from byproduct Cp$_2$ZrCl$_2$ by washing or fractional crystallization.
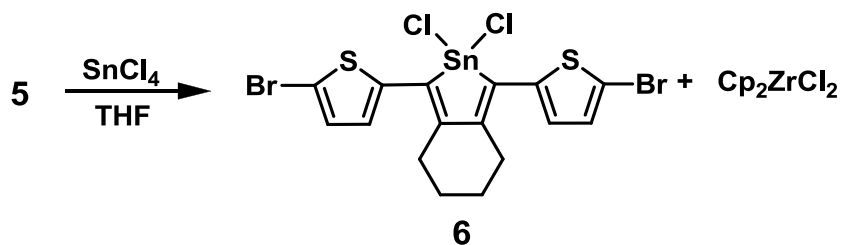
Scheme 2.9 Metallacycle transfer of **5** with SnCl$_4$.

Since solution processablity has essential impacts on the properties of final solar cell devices, the poor solubility of **5** and its derived main group analogues, and the difficulty of separation of target products from the Cp_2ZrCl_2 were seen as significant drawbacks that needed to be overcome.

2.2.3 Enhancing the solubility of a hybrid-thiophenezirconacyclopentadiene precursor

As mentioned, the low solubility of **5** and the main group heterocycle that were prepared from this precursor caused difficulties during purification. Therefore, we decided to improve the solubility of our zirconacycle precursors by incorporating a solublizing hexyl group onto each of the thiophene rings (Scheme 2.10). Following similar chemistry as before, the desired thiophene-capped bis(alkyne) precursor **7** was prepared in three steps, starting from commercially available 3-hexylthiophene. The presence of the added hexyl groups on the thiophene alkyne precursor made the Sonogashira cross-coupling of 2-bromo-3-hexyl-5-iodothiophene with 1,7-octadiyne more difficult. For example, when two equivalents of 2-bromo-3-hexyl-5-iodothiophene were combined with one equivalent of 1,7-octadiyne under the same conditions as in Scheme 2.8, we obtained a mixture of products containing both **7** and significant amount of the mono-substituted diyne.
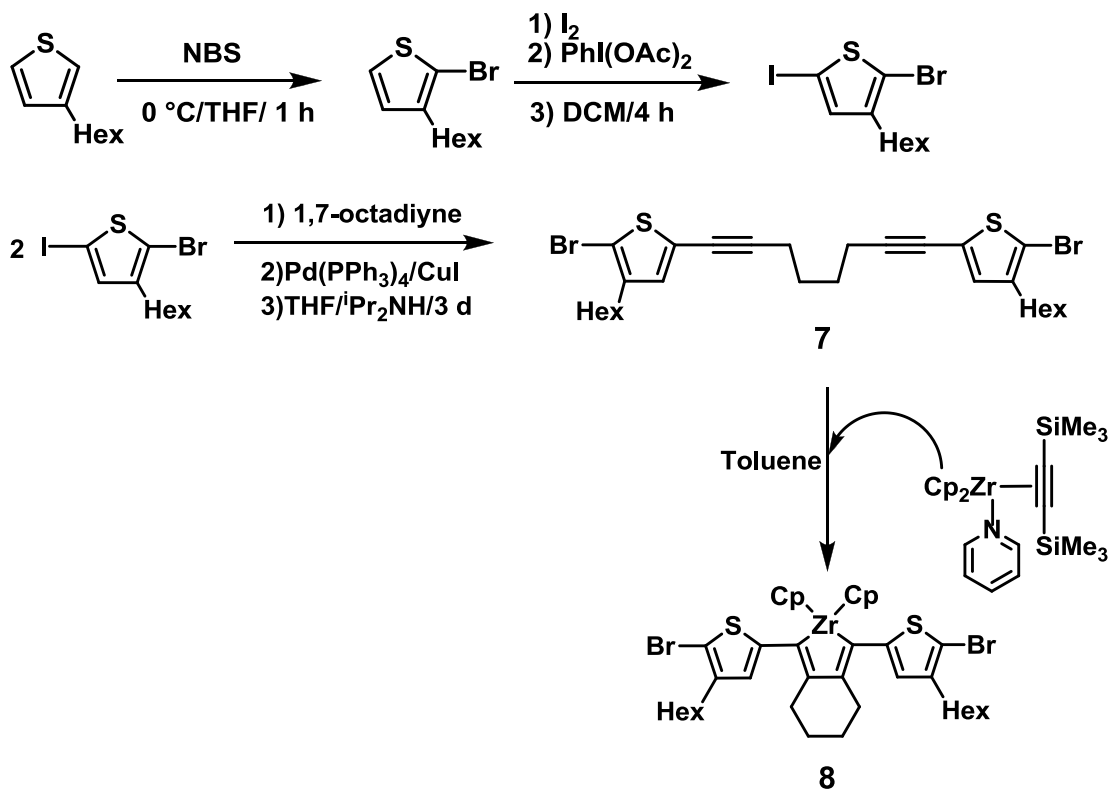
Scheme 2.10 Synthesis of the hexyl-functionalized soluble zirconacyclopentadiene **8**.

In order to increase the yield of **7**, the reaction was performed using an excess amount of 2-bromo-3-hexyl-5-iodothiophene (3 equivalents per molecule of 1,7-octadiyne) with a higher catalyst loading (5 mol% vs. the original amount 2 mol%) and at an elevated temperature at 80 °C for three days. After work-up and purification by column chromatography, compound **7** was obtained as a pale yellow oil. ^{1}H and ^{13}C{^{1}H} NMR spectroscopy (Figure 2.2 and 2.3) provided evidence for the formation of the thiophene-capped diyne **7**. ^{1}H NMR spectroscopy showed a singlet resonance due to a thiophene-bound hydrogen atom at 6.81 ppm along with expected resonances for the hexyl and bridging methylene (CH$_2$) groups. In addition, two well-resolved ^{13}C {^{1}H}

NMR resonances at 94.7 and 73.8 ppm were observed that were assigned to distinct two alkynyl carbon environments.
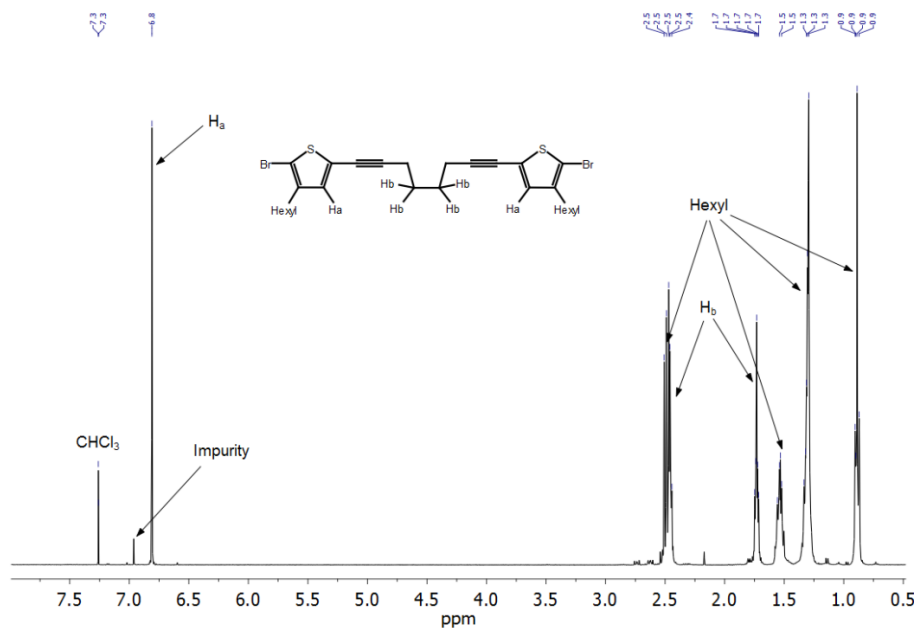
Figure 2.2 ^{1}H NMR spectrum of **7**.
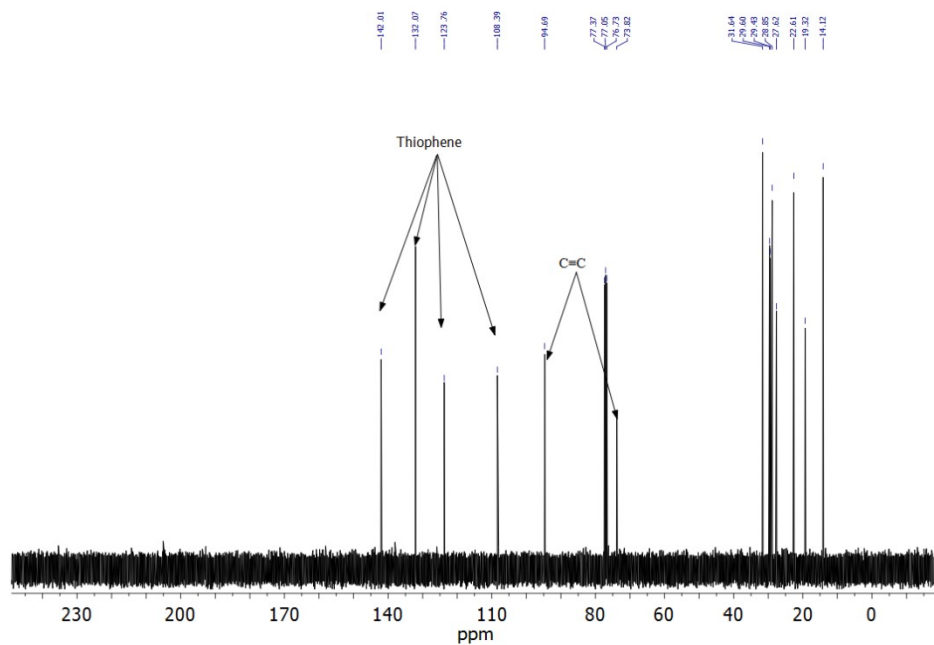
Figure 2.3 ^{13}C{^{1}H} NMR spectrum of **7**.

Following similar chemistry as used to prepare **5**, Rosenthal's reagent was then reacted with **7** to form the zirconacyclopentadiene complex **8**. Compared with compound **5**, compound **8** exhibits superior solubility in common organic solvents, and pure **8** could be recrystallized from hexanes (-30 °C) to give **8** as red crystals. The molecular structure of **8** was determined by single crystal X-ray crystallography (Figure 2.4), and the associated crystallographic data are summarized in Table 2.1 at the end of this chapter. The crystal structure of **8** unambiguously confirmed the formation of zirconacyclopentadiene heterocycle fused with a 6-membered alkane ring. The planarity of zirconacyclopentadiene ring is proved by two set of torsion angles: 0.3(2)° for C(8)—Zr—C(7)—C(1), and -3.9(2)° for C(7)—Zr—C(8)—C(2). Surprisingly, the two thiophene groups and the zirconacyclopentadiene rings are not coplanar with torsion angles of -35.6(3)° [Zr—C(7)—C(11)—S(1)] and 94.5(3)° [Zr—C(8)—C(21)—S(2)] respectively. The 6-membered ring that is linked to the zirconacycle showed significant twisting of the $(CH_2)_4$ group with torsion angles of 154.5(3)° [C(7)—C(1)—C(6)—C(5)] and 159.5(3)° [C(8)—C(2)—C(3)—C(4)].

Figure 2.4 Molecular Structure of **8** with thermal ellipsoids presented at a 20% probability level. All hydrogen atoms have been omitted for clarity. Selected bond length (Å): Zr—C(7), 2.275(3); Zr—C(8), 2.255(3); C(7)—C(1), 1.370(4); C(8)—C2, 1.358(4); C(1)—C(2), 1.502(4). Selected bond angles (deg): C(7)—Zr—C(8), 77.24(10); Zr—C(7)—C(1), 111.8(2); Zr—C(8)—C(2), 112.40(19); C(8)—C(2)—C1, 119.3(3); C(2)—C(1)—C(7), 118.8(3).

2.2.4 Synthesis of germole and stannoles analogues via metallacycle transfer from compound 8

Germoles and stannoles have received much less attention as a building block for

conjugated polymers as compared to their group 16 element counterparts (*e.g.* thiophene).

However, according to studies conducted by Yang[16] and Brabec[17], replacing the carbon atom by a silicon atom in a conjugated ring enhances the crystallinity of the material. Following those encouraging results, heteroles from group 14 elements has been studied more actively than in the past, including the synthesis of germacyclopentadienes, stannacyclopentadienes, and their derivatives. To summarize recent studies,[18] those papers show that the longer C—E (E = Si, Ge, Sn) in the germole or stannoles rings allow for better π—π intermolecular interactions, which, in turn, can lower the band gap. Therefore, it can then be interesting to incorporate Ge and Sn into the conjugated rings using the strategy introduced in Section 2.2.3.

2.2.4.1 Preparation of germoles via zirconium-mediated metallacycle transfer

Based upon the good solubility of **8**, we performed metallacycle transfer chemistry between this zirconacycle and GeCl$_4$ (Scheme 2.11). This reaction proceeded quite readily when an excess of GeCl$_4$ (2 equivalents) was used. The byproduct, Cp$_2$ZrCl$_2$, could also be quantitatively removed from product **9** in hexanes by filtering the reaction mixture through silica gel. The removal of Cp$_2$ZrCl$_2$ from **9** was confirmed by ^{1}H NMR spectroscopy. The resulting dichlorogermole was isolated in 70% yield as a red oil and characterized by ^{1}H, ^{13}C{^{1}H} NMR and UV-vis spectroscopy.
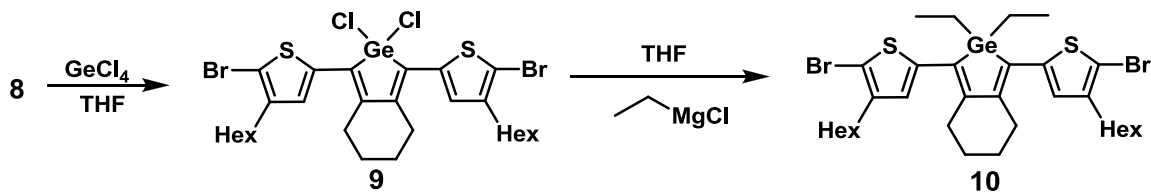
Scheme 2.11 Synthesis of the germole analogue **10** starting from zirconacycle **8**.

In order to form an air-stable germole, treatment of **9** with the Grignard reagent EtMgCl in THF was conducted at ambient temperature and afforded the diethylgermole analogue **10**. Pure **10** was obtained by column chromatography with hexanes as the eluent; however, the product yield was quite low (19%). Formation of a germole with ethyl groups attached was confirmed by NMR spectra analysis. The ^{1}H NMR spectrum of **10** shows quartet and triplet resonances due to the attached ethyl group (Figure 2.5); moreover, comparing the ^{13}C{^{1}H} NMR spectra of **10** with a known germole heterocycle, 1,1-dimethyl-3,4-trimethylene-2,5-di(2-thienyl)germole, also provided diagnostic evidence about the incorporation of ethyl group onto Ge. We can clearly observe two signals downfield at 9.1 and 8.2 ppm in Figure 2.6 due to the ethyl group, while similar resonances at 9.2 and 8.3 ppm were seen for the ethyl group in 1,1-dimethyl-3,4-trimethylene-2,5-di(2-thienyl)germole.[19]
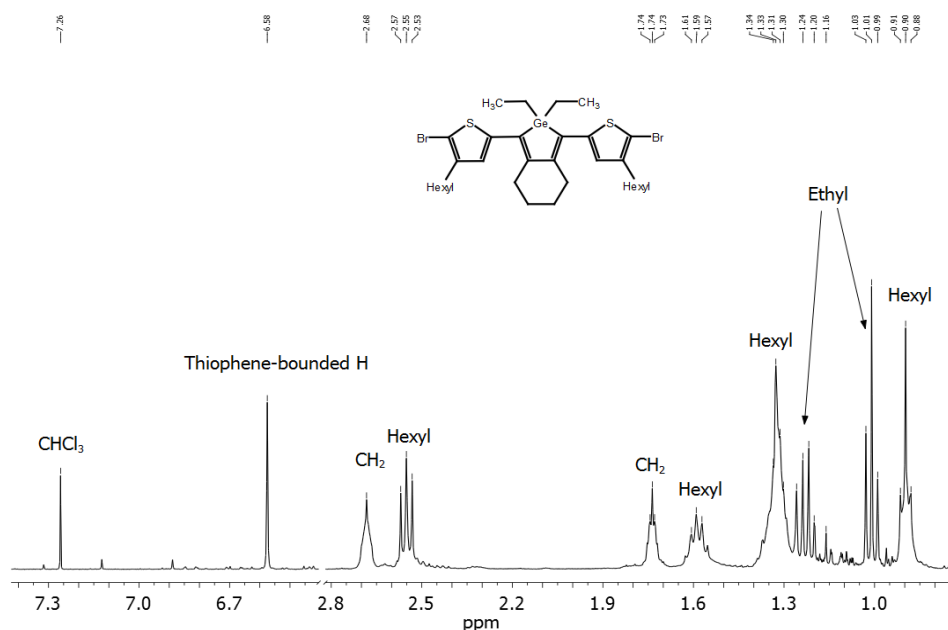
Figure 2.5 ^{1}H NMR spectrum of compound **10**.
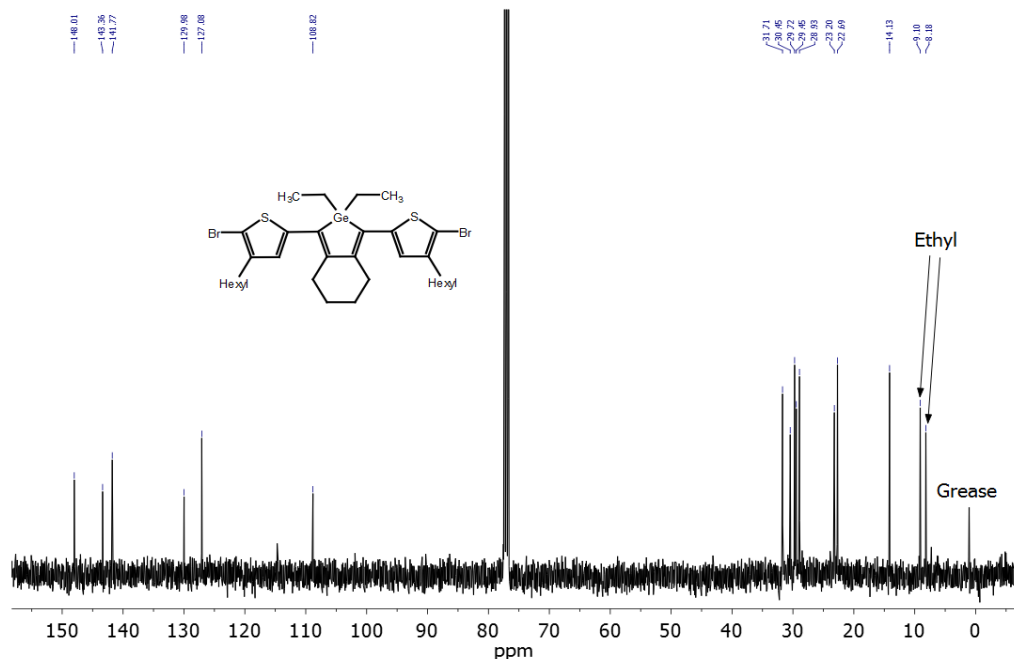
Figure 2.6 $^{13}C\{^1H\}$ NMR spectrum of compound **10**.

2.2.4.2 Preparation of stannoles via zirconium-mediated metallacycle transfer

Attempts to react dimethyltin dicholride Me$_2$SnCl$_2$ with the zirconacyclopentadienes, **3** or **5,** unfortunately did not give well-defined products (Scheme 2.12) according to ^{1}H NMR spectroscopy. Copper (I) chloride has been reported to be able to promote metallacycle transfer chemistry between zirconacycles and tin halides.[20] However, addition of CuCl did not lead to satisfactory reactions based on the ^{1}H NMR spectrum of crude product.
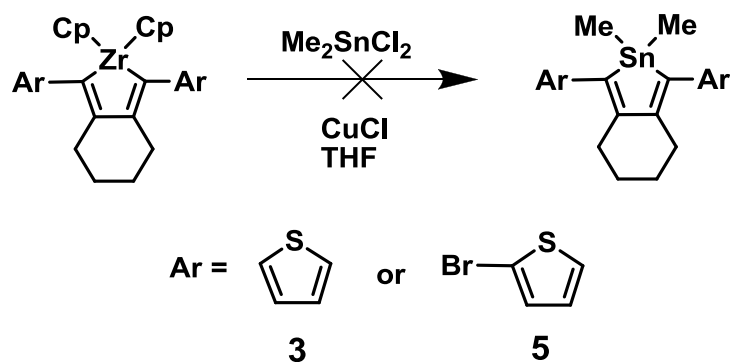
Scheme 2.12 Unsuccessful attempts at preparing organostannacycles.

Fortunately, SnCl$_4$ reacted smoothly with the zirconacyclopentadiene **8** (Scheme 2.13). As the reaction proceeded, the color of reaction mixture turned from its original dark-red color to orange. In addition, ^{1}H NMR spectroscopy analysis of the crude product after work-up showed an upfield shift of the Cp resonance from 6.24 ppm in **8** to 6.49 ppm (due to formation of the byproduct, Cp$_2$ZrCl$_2$). This observation from ^{1}H NMR spectroscopy provided evidence that metallacycle transfer with SnCl$_4$ had proceed. Unlike compound **6** which exhibits poor solubility in common organic solvents, the hexylthiophene-functionalized zirconacyclopentadiene, **8**, and stannacycles analogue **11** obtained after metallacycle transfer both showed good solubility in hexanes, in which Cp$_2$ZrCl$_2$ is sparingly soluble. Thus, **11** can be readily separated from Cp$_2$ZrCl$_2$ after filtration. In order to render the stannacycle more stable to moisture, EtMgCl was then reacted with **11**; however, we were unable to obtain clean alkylation chemistry of **11** despite multiple attempts.
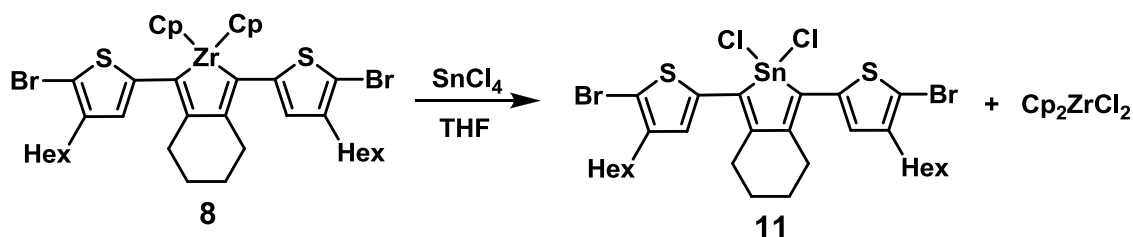
Scheme 2.13 Synthesis of the stannacycles **11** via metallacycle transfer chemistry.

2.2.5 Synthesis of selenophene via metallacycles transfer from zirconacycle 8

Selenium dichlororide, $SeCl_2$, is an promising reagent for metallacycle transfer; however; selenium dihalides in pure form can undergo dispropotionation rapidly:

$$3\ SeX_2 \rightleftharpoons Se_2X_2 + SeX_4$$

$$X = Cl\ or\ Br \tag{1}$$
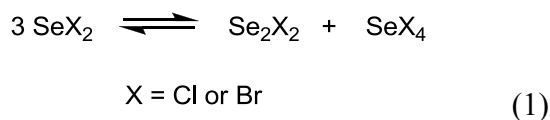
Therefore, it is a challenge to prepare pure, stable $SeCl_2$. Maaninen and coworkers developed a convenient method to generate $SeCl_2$ from Se powder and SO_2Cl_2, and the resulting $SeCl_2$ product is then dissolved in THF to give a temporarily stable solution. When zirconacyclopentadiene **8** was reacted with freshly made $SeCl_2$ at room temperature, the selenophene **12** was obtained (Scheme 2.14). Promising evidence for the formation of **12** was observed by ^1H and $^{13}C\{^1H\}$ NMR spectroscopy. However, **12** decomposed to a black unidentifiable mixture after standing at room temperature in solution of $CDCl_3$ within one hour. In addtion, isolated **12** underwent the same decomposition in the condensed phase as noted by a color change from orange to black accompanied by the the formation of a solid (from oily **12**).
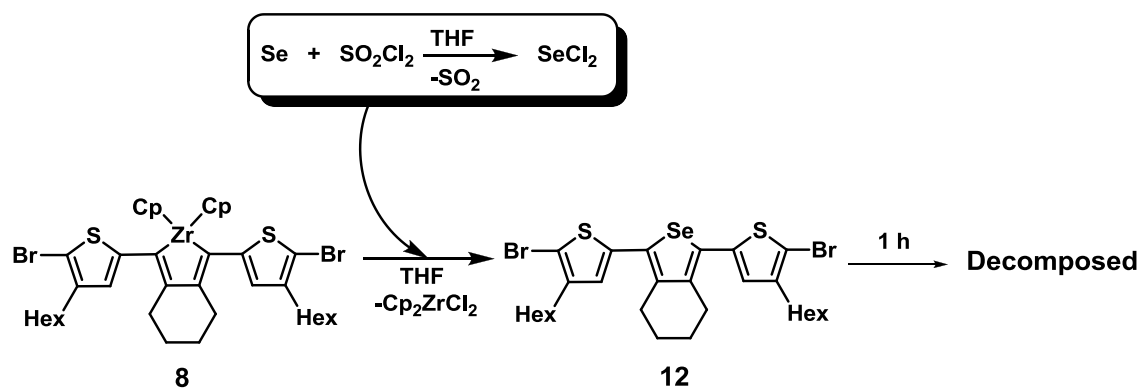
Scheme 2.14 Synthesis of the selenophene **12** from **8**.

2.2.6 Synthesis of stable selenophene from the modified zirconacycle 14 and its polymerization

As mentioned previously, the selenophene **12** decomposed to a black mixture over time in both solution and in the condensed phase. In order to investigate whether the presence of terminal bromide groups played a role in the decomposition of the selenophene-dithiophene analogue **12**, we decided to prepare a related compound whereby the capping bromine groups were replaced by hydrogen (Scheme 2.15). The diyne **13** was prepared from 1,7-octadiyne and excess 2-bromo-3-hexylthiophene (1:3 ratio) to encourage the formation of a disubstituted product. Separation of **13** from unreacted 2-bromo-3-hexylthiophene was facile through column chromatography due to distinct R$_f$ values of each compound.
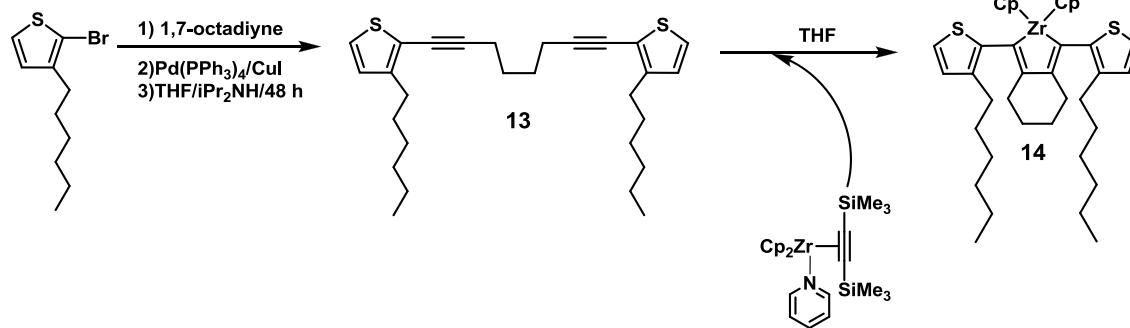
Scheme 2.15 Synthesis of the thiophene-terminated zirconacyclopentadiene without terminal bromide groups.

Although **13** did not contain a terminal bromide group, Rosenthal's zirconocene reagent was used as a Cp$_2$Zr source, instead of Negishi's reagent, as higher yields are generally obtained. The reaction proceeded similarly as with the formation of **8**, but longer reaction times, up to three days, were required in order to give high yields of the zirconacycle **14**.

Pure **14** was obtained as red crystals by cooling a solution of **14** in hexanes to -30 °C. The molecular structure was determined by single-crystal X-ray crystallography (Figure 2.7), and the detailed crystal data are summarized in Table 2.1 at end of this chapter. As in **8**, a planar zirconacyclopentadiene ring is present in **14**. The molecular structure of **14** exhibits a lack of co-planarity between the zirconacycle and the two neighboring thiophene rings as shown by torsion angles of 71.3(3)° [C(1)—C(7)—C(11)—C(12)] and -70.5(4)° [C(2)—C(8)—C(21)—C(22)]. Interestingly, the two thiophene rings are orientated in a similar fashion with the sulfur atoms pointing away from the Zr center. Compared with structure of **8**, the hexyl groups in **14** are attached at inner positions of each thiophene ring, which greatly lessen the distance between the two hexyl groups.

Steric and electronic repulsion between hexyl groups twist the two thiophene rings in two opposite directions and disrupt the coplanarity between zirconacycle and thiophene rings.
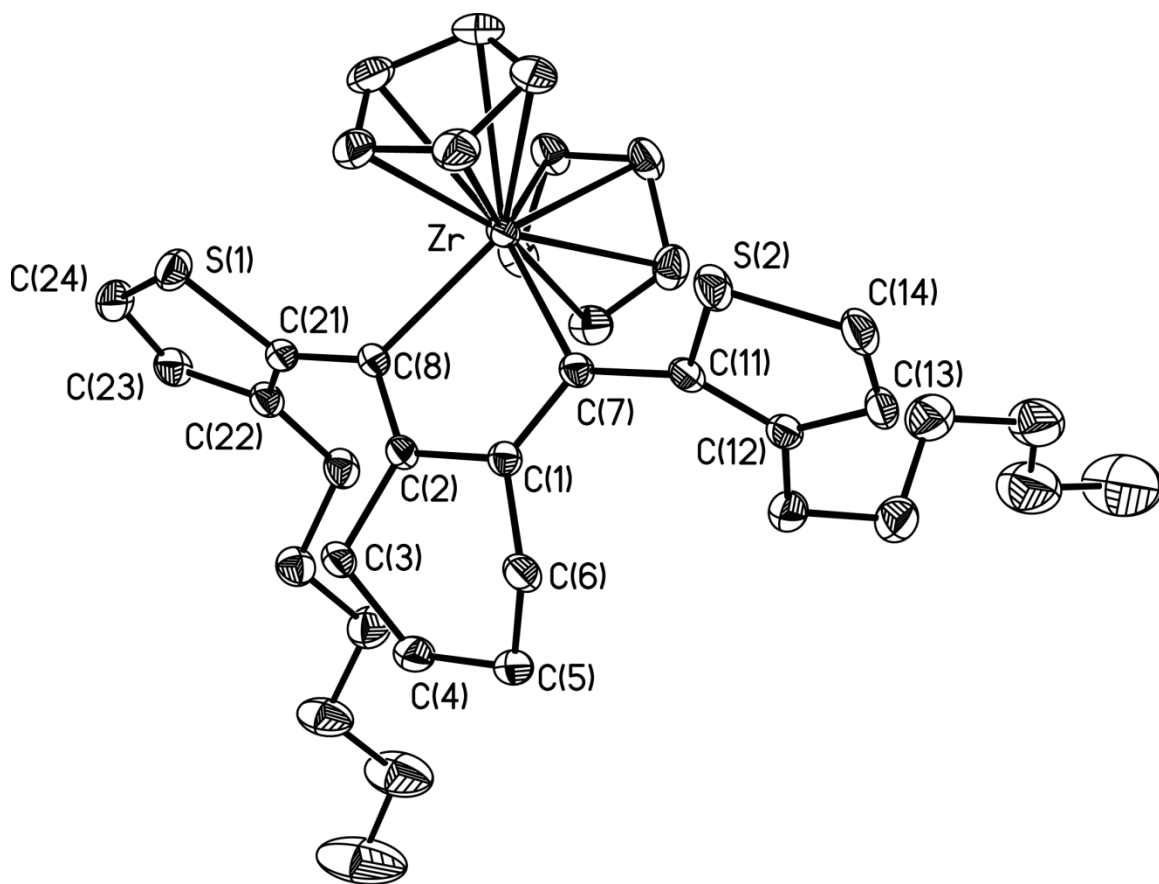
Figure 2.7 Molecular structure **14** with thermal ellipsoids presented at a 20% probability level. All hydrogen atoms have been omitted for clarity. Selected bond lengths (Å): Zr—C(7), 2.261(2); Zr—C(8), 2.264(2); C(2)—C(8), 1.354(3); C(1)—C(7), 1.361(3); C(1)—C(2), 1.496(3). Bond angles (deg): C(7)—Zr—C(8), 80.59(8); Zr—C(7)—C(1), 107.95(15); C(7)—C(1)—C(2), 121.6(2); C1—C(2)—C(8), 122.01(19); C(2)—C(8)—Zr, 107.84(15)

The reaction of the modified zirconacycle **14** with in situ generated SeCl$_2$ proceeded smoothly at room temperature, and pure **15** could be readily isolated in pure form as a pale yellow oil (Scheme 2.16). Compound **15** is stable at room temperature both in solution and in the condensed phase; however, it still does not contain functional groups

required for polymerization. Therefore, **15** was brominated at the terminal 5-position of the thiophene rings using N-bromosuccinimide (NBS) to give **16** as a pale yellow oil (Scheme 2.16). While the selenophene analogue **12** decomposed quickly, both of compounds **15** and **16** exhibit stability for indefinite periods of time and superior solubility in common organic solvents, which makes **16** an ideal monomer to polymerize in a later step.

Yamamoto coupling of **16** with stoichiometric Ni(COD)$_2$ was performed to yield a new thiophene-selenophene hybrid polymer (**PM3**). Polymer **PM3** remained soluble in the toluene reaction mixture and was isolated as brown solid by precipitation into methanol. The molecular weight of **PM3** was determined by the GPC (Mw = 63,600 g/mol, PDI = 1.56). The thermal stability was measured by TGA, which showed a weight loss of 5% at 190 °C.
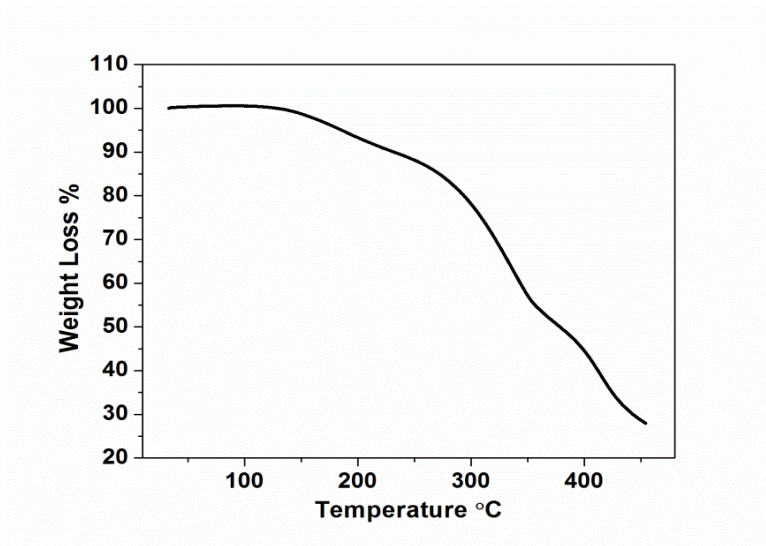
Figure 2.8 TGA data for **PM3**
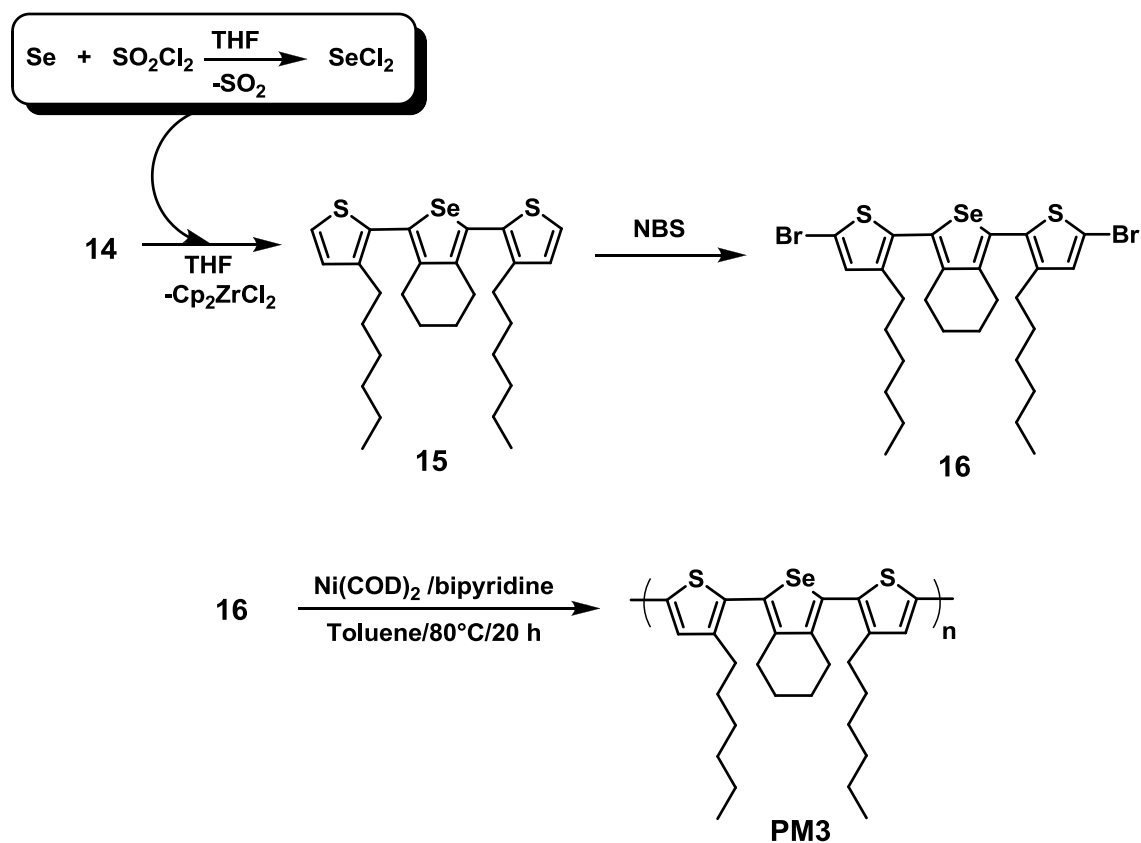
Scheme 2.16 Synthesis of the selenophene-containing polymer **PM3**.

Furthermore, it was also of interest to investigate how the presence of selenium in a polymer affected the optical band gap. The butadiene-linked dithiophene, **17**, was prepared by adding an aqueous HCl solution to zirconacycle precursor **14** (Scheme 2.17). Although compound **17** does not contain any heavy main group elements, it can be viewed as a building unit for an organic thiophene polymer.
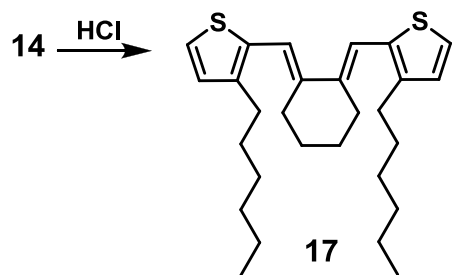
Scheme 2.17 Hydrolysis of **14** to give **17**.
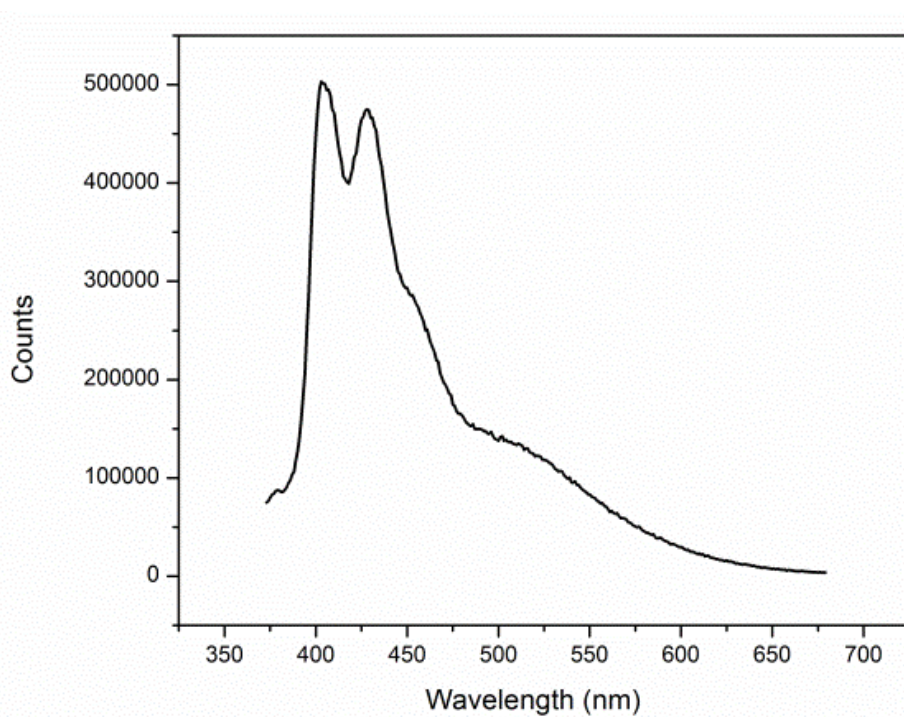
Figure 2.9 Fluorescence spectrum of **PM3**.
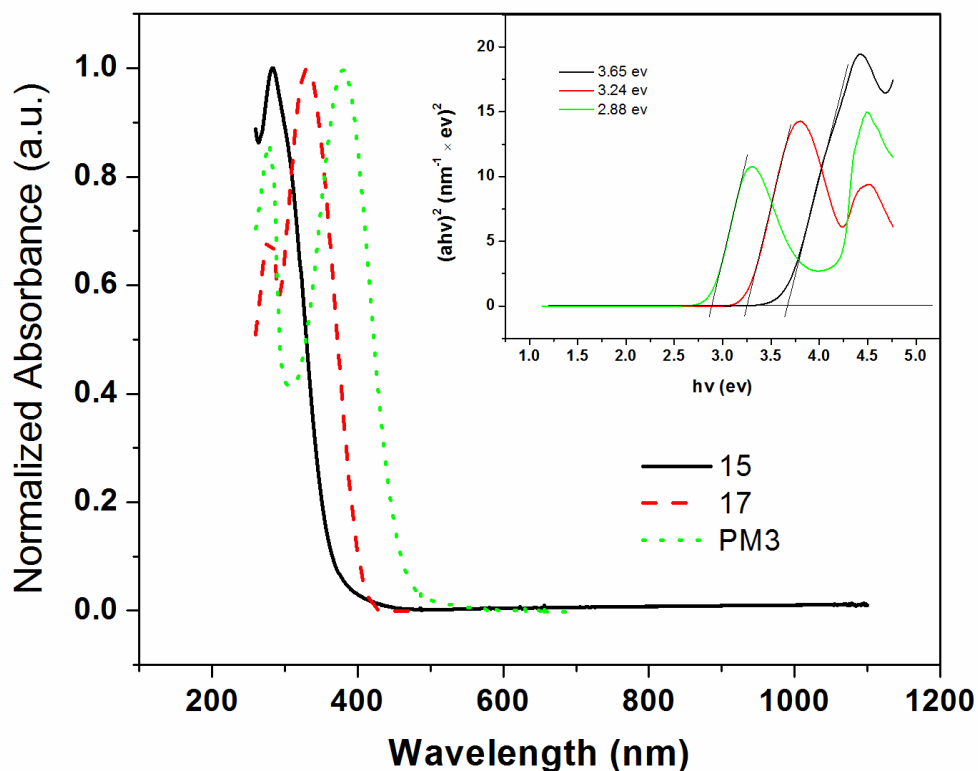
Figure 2.10 Comparison of UV-vis spectra for compound **15**, **17**, and **PM3**.

The fluorescence spectrum of **PM3** in Figure 2.9 has shown two peaks at 405 nm and 430 nm, which are fluorescence emissions, caused electron relaxation from the higher energy state to different vibrational energy states of ground state S_0. Preliminary optical study includes **PM3**, monomer **15**, and the hydrolyzed monomer **17**. UV-vis spectroscopy was performed, and the results are shown in Figure 2.10. By comparing the UV-vis spectra of **PM3**, **15**, **17** with normalized absorbance, we can see that the λ_{max} of **PM3** is red-shifted with respect to the λ_{max} (382 nm) value of monomer **15** (283 nm), implying an increase in the conjugation length after the polymerization. Without the

presence of Se in the heterocycle, red-shifted λ_{max} spectra were observed for the hydrolyzed compound **17** compared with presence of a selenophene ring in **15**. The band gaps were calculated based on λ_{onset} from UV-vis spectra, where the band gaps for **PM3**, **17**, **15** increased in the order: 2.88 eV, 3.24 eV, and 3.65 eV, respectively.

2.3 Conclusions

Despite initial unsuccessful attempts, a new convenient synthetic route for the rapid preparation of conjugated polymers has been developed in this chapter. For example, the synthesis of the selenophene/thiophene hybrid polymer **PM3** was possible in only five steps, and with this general strategy, the incorporation of various different elements into conjugated polymer arrays is feasible. This study also demonstrated the advantage of isolating the zirconacycles before metallacycle transfer, which enable us to conveniently study the reactivity of these zirconacycles in order to find the optimal conditions for metallacycle transfer chemistry.

In all, we attempted to construct conjugated polymers based on three elements, Sn, Se, and Ge via metallacycle transfer. Whereas efforts towards obtain stable analogues of stannoles were fruitless, the germole **10** and selenophene **15** were successfully prepared from two readily prepared zirconacyclopentadienes, **7** and **14**, respectively. While we were unable to obtain significant quantities **10** for polymerization, the polymerization of **16** yields an alternate thiophene/selenophene polymer (**PM3**) in high yield. The presence of hexyl groups in **PM3** makes these material soluble in common organic solvents, which should enable solution coating methods such as spin-coating and inject printing to be realized. In addition, initial optical data were obtained for compounds **15**, **17**, and

polymer **PM3**. Surprisingly, the incorporation of Se into monomer **15** results in a blue shift of 50 nm compared to the hydrolyzed metal-free compound **17**. One the other hand, polymerization of **16** did lead to significant red shit of UV-vis spectrum compared to monomeric **17**. The presence of selenophene units in a polymer does lead to low band gap (2.88 eV). However, the band gap in **PM3** is not still low enough to compete with other leading conjugated polymers for solar cells, although we have yet to measure the band gap of an annealed film of **PM3**.

Even though **PM3** does not seem suitable for high performance BHJSCs, we anticipate that this synthetic route will still be useful for the synthesis of a variety of new conjugated polymers. Further studies can be focused on synthesis of stable stannoles from zirconacycle **8** or improving the yield of the germole analogue **10**. Also, the use of stable selenophene **16** as a building block to copolymerize with other conjugated systems is under investigation.

2.4 Experimental Section

2.4.1 Materials and Instrumentation

General All reactions were performed by applying standard Schlenk and glovebox techniques under a nitrogen atmosphere. Solvents were all dried and degassed using a Grubbs-type solvent purification system manufactured by Innovative Technology, Inc.[21], and stored under an atmosphere of nitrogen prior to use. 1,7-octadiyne was purchased from GFS Chemicals; 2-iodothiophene was purchased from Alfa Aesar; 3-hexylthiophene was purchased from Ontario Chemical Inc., and all other chemicals were purchased from Aldrich. All of chemicals were used as received without further purification except triethylamine and diisopropylamine. Triethylamine and diisopropylamine were freshly distilled under nitrogen from potassium hydroxide. 2,5-bis(1-hexynyl)thiophene,[14a] $Cp_2Zr(pyridine)(Me_3SiC{\equiv}CSiMe_3)$, [22] [a] 1,8-di(thiophen-2-yl)octa-1,7-diyne, 2-bromo-5-iodothiophene, and 2-bromo-3-hexyl-5-iodothiophene[22b] were prepared according to literature procedures. ^1H, $^{13}C\{^1H\}$ NMR spectra were recorded on a Varian Inova-400 spectrometer and referenced externally to $SiMe_4$ (^1H, $^{13}C\{^1H\}$). Elemental analysis were performed by the Analytical and Instrumentation Laboratory at the University of Alberta. Mass spectra were obtained on an Agilent 6220 spectrometer. Melting points were obtained in sealed glass capillaries under nitrogen using a MelTemp melting point apparatus and are uncorrected.

2.4.2 Single-crystal X-ray structure determination of 8 and 14

X-ray Crystallography. Crystals of appropriate quality for X-ray diffraction studies were removed from a vial (in a glove box) and immediately covered with a thin layer of hydrocarbon oil (Paratone-N). A suitable crystal was then selected, attached to a glass fiber, and quickly placed in a glass vial. All data were collected using a Bruker APEX II CCD detector/D8 diffractometer using Mo Kα radiation. The data were corrected for absorption through Gaussian integration from indexing of the crystal faces. Structures were solved using the direct methods programs SHELXS-97, and refinements were completed using the program SHELXL-97. Non-hydrogen atoms are represented by Gaussian ellipsoids at the 20% probability level. All hydrogen atoms in compound **8** are shown with arbitrarily small thermal parameters; all other hydrogens are not shown.

2.4.3 Synthetic Details

Preparation of Cp$_2$Zr-2,5-di(thienyl)(CH$_2$)$_4$ (3). To a solution of Cp$_2$ZrCl$_2$ (0.76 g, 2.60 mmol) in 30 mL of THF was added ^{n}BuLi (2.03 mL, 2.5 M in hexanes, 5.07 mmol) at -78 °C. After the solution was stirred for 3 h at -78°C, bis-p-thienyl-1,6-heptadiyne (0.70 g, 2.60 mmol) in 10 mL of THF was added dropwise. The resulting solution was allowed to warm to room temperature and stirred for an additional 4 h. While stirring, the solution gradually turned crimson from yellow color. The volatiles were removed under reduced pressure, and the residue was redissolved in 20 mL of toluene and the solution was filtered through Celite. The resulting filtrate was collected and the solvent was removed under vacuum to give **3** as a red free-flowing powder (0.59 g, 46%). ^{1}H NMR (400 MHz, CDCl$_3$): δ 7.12 (dd, $^3J_{HH}$ = 5.2, $^4J_{HH}$ = 1.2 Hz, 2H, thienyl-H), 6.97 (dd, $^3J_{HH}$ = 5.2, $^4J_{HH}$

= 3.6 Hz, 2H, thienyl-H), 6.24 (dd, $^3J_{HH}$ = 7.6, $^4J_{HH}$ = 3.6 Hz, 2H, thienyl-H), 6.23 (s, 10H, Cp), 2.46 (t, $^3J_{HH}$ = 6.8 Hz, 4H, -CH$_2$-), 1.57 (m, 4H, -CH$_2$-). ^{13}C{^{1}H}NMR (100 MHz, CDCl$_3$): δ 177.0, 150.0, (ZrC=C), 142.0, 127.0, 122.6, 121.0 (thiophene), 111.9 (Cp), 29.6, 23.6. (CH$_2$). UV-vis (CH$_2$Cl$_2$, nm, log ϵ): 399, 3.8. Anal. Calcd. for C$_{26}$H$_{24}$S$_2$Zr: C, 63.49; H, 4.92; S, 13.04. Found: C, 61.03; H, 5.00; S, 10.52.

Preparation of 1,8-di(5-bromothiophen-2-yl)octa-1,7-diyne (4). 2-Bromo-5-iodo-thiophene (4.00 g, 13.8 mmol), 1,7-octadiyne (0.73 g, 6.9 mmol), Pd(PPh$_3$)$_4$ (380 mg, 0.345 mmol), and CuI (64 mg, 0.345 mmol) were dissolved in 80 mL of THF under nitrogen, and diisopropylamine (20 mL) was then added. The reaction mixture was allowed to stir at room temperature for 3 days, resulting in the formation of a white precipitate. The reaction mixture was filtered, and the filtrate was collected and diluted with 100 mL of hexanes and washed with a 10% NH$_4$OH (100 mL) solution, water, 2 N HCl (100 mL), water, and brine, and then dried over MgSO$_4$. The solvent was then removed under vacuum, and the crude product was purified by column chromatography (silica gel, eluent: hexanes). Pure **4** was obtained as a white solid (0.92 g, 31%). ^{1}H NMR (400 MHz, CDCl$_3$): δ 6.89 (d, $^3J_{HH}$ = 4.0 Hz, 2H, thienyl-H), 6.86 (d, $^3J_{HH}$ = 4.0 Hz, 2H, thienyl-H), 2.47 (m, 4H, -CH$_2$-), 1.74 (m, 4H, -CH$_2$-). ^{13}C{^{1}H}NMR (100 MHz, CDCl$_3$): δ 131.4, 129.8, 125.9, 111.6 (thiophene), 95.0, 73.5 (C≡C) 27.6 (CH$_2$), 19.3 (CH$_2$). Mp (°C): 50-52. HR-MS (EI): m/z; Calcd. 427.87267. Found 427.87259 (Δ ppm = 0.2). Anal. Calcd. for C$_{16}$H$_{12}$S$_2$Br$_2$: C, 44.88; H, 2.82; S, 14.98. Found: C, 44.81; H, 2.91; S, 14.67.

Preparation of Cp$_2$Zr-2,5-di(2-bromo-thienyl)(CH$_2$)$_4$ (5). Compound **4** (0.54 g, 1.27 mmol) and Cp$_2$Zr(pyr)(Me$_3$SiC≡CSiMe$_3$) (0.57 g, 1.27 mmol) were dissolved in 15 mL

71

toluene. The mixture was allowed to stir for 14 h at 60 °C and then filtered through Celite. The filtrate was collected, and the solvent was then removed under reduced pressure to afford **5** as a dark-red solid (0.82 g, 81%). ^{1}H NMR (400 MHz, CDCl$_3$): δ 6.89 (d, $^3J_{HH}$ = 3.6 Hz, 2H, thienyl-H), 6.24 (s, 10H, Cp), 5.89 (d, $^3J_{HH}$ = 4.0 Hz, 2H, thienyl-H), 2.41 (t, $^3J_{HH}$ = 6.8 Hz, 4H, -CH$_2$-), 1.56 (m, 4H, -CH$_2$-). ^{13}C{^{1}H}NMR (100 MHz, CDCl$_3$): δ 176.5, 151.3 (ZrC=C), 142.8, 129.7, 121.5, 108.9 (thiophene), 112.1 (Cp), 29.7 (CH$_2$), 23.4 (CH$_2$). UV-vis (CH$_2$Cl$_2$, nm, log ε): 400, 4.1. Anal. Calcd. for C$_{26}$H$_{22}$Br$_2$S$_2$Zr: C, 48.07; H, 3.41; S, 9.87. Found: C, 49.11; H, 3.64, S 9.62.

Preparation of 1,8-di(5-bromo-4-hexylthiophen-2-yl)octa-1,7-diyne (7). 2-Bromo-3-hexyl-5-iodothiophene (2.36 g, 6.34 mmol), 1,7-octadiyne (0.22 g, 2.11 mmol), Pd(PPh$_3$)$_4$ (105 mg, 0.106 mmol) and CuI (23 mg, 0.106 mmol) were dissolved in 50 mL of THF under N$_2$, and 15 mL of diisopropylamine was then added to this mixture under N$_2$. The resulting mixture was stirred at 60 °C for 3 days. A large amount of white precipitate formed during the reaction, and the reaction mixture was filtered. The filtrate was diluted with 50 mL of hexanes and washed with 100 mL of 10% NH$_4$OH solution, water, 2 N HCl, water, and brine respectively, and then dried over MgSO$_4$. The solvent was removed under reduced pressure to give the crude product as a brown oil. The product was purified by column chromatography (silica gel, 40 mL of hexanes first, then hexanes:ethyl acetate = 20:1, 40 mL). The first fraction contained the starting material 2-bromo-3-hexyl-5-iodothiophene, while the second fraction consisted of pure **7**. After removing the volatiles, **7** was isolated as a pale yellow oil (0.35g, 28%). ^{1}H NMR (400 MHz, CDCl$_3$): δ 6.81 (s, 2H, thienyl-H), 2.49 (t, $^3J_{HH}$ = 7.2 Hz, 4H, -CH_2-), 2.47 (m, 4H,

C≡C -CH₂), 1.73 (m, 4H, C≡C-CH₂-CH₂), 1.53 (m, 4H, -CH₂-), 1.29 (m, 12H, -CH₂CH₂CH₂-), 0.89 (t, $^3J_{HH}$ = 7.2 Hz, 6H, -CH₃). ^{13}C{^{1}H}NMR (100 MHz, CDCl₃): δ 142.0, 132.0, 123.7, 108.4 (thiophene), 94.7, 73.8 (C≡C), 31.6, 19.3 (C=C), 29.5, 29.4, 28.8, 27.6, 22.6, 14.1 (hexyl). HR-MS (EI): m/z; Calcd.: 596.0605, Found: 596.0674 (Δ ppm = -11.6). Anal. Calcd. for C₂₈H₃₆Br₂S₂: C, 56.38; H, 6.08; S, 10.75. Found: C, 56.34; H, 6.10; S, 10.83.

Preparation of Cp₂Zr-2,5-di-(2-bromo-3-hexylthiophenyl)(CH₂)₄ (8). Compound **7** (0.49 g, 0.94 mmol) and Cp₂Zr(pyr)(Me₃SiC≡CSiMe₃) (0.44 g, 0.94mmol) were dissolved in 15 mL THF, and the resulting mixture was allowed to stir overnight to give a dark red solution. The solvent was removed under reduced pressure, and the residue was extracted with 5 mL of hexanes, and the resulting solution was filtered through Celite. The filtrate was placed in -30 °C freezer for 24 h, which resulted in the formation of dark red crystals of **8**. The crystals were subsequently isolated and dried under vacuum (0.19 g, 29%). ^{1}H NMR (400 MHz, CDCl₃): δ 6.24 (s, 10H, Cp), 5.85 (s, 2H, thienyl-H), 2.51 (t, $^3J_{HH}$ = 10.0 Hz, 4H, -CH₂, hexyl), 2.41 (t, $^3J_{HH}$ = 8.4 Hz, 4H, -CH₂, 6-membered ring), 1.56 (m, 4H, -CH₂, 6-membered ring), 1.34 (m, 12H, -CH₂CH₂CH₂-, hexyl), 0.91 (m, 6H, -CH₃, hexyl). ^{13}C{^{1}H}NMR (100 MHz, CDCl₃): δ 176.5, 149.0, (Zr-C=C-) 142. 5, 141.7, 122.3, 105.9 (thiophene), 112.0 (Cp), 31.7, 29.8, 29.7, 29.6, 28.9, 23.5, 22.7, 14.2. UV-vis (hexanes, nm, log ε), 291, 4.22; 328, 4.21. Anal. Calcd. for C₃₈H₄₆Br₂S₂Zr: C, 55.80; H, 5.67; S, 7.84. Found: C, 55.90; H, 5.87; S, 7.77.

Preparation of dichlorogermole-2,5-di(2-bromo-3-hexylthiophenyl)(CH$_2$)$_4$ (9). To a 5 mL THF solution of compound **8** (0.148 g, 0.181 mmol) was added an excess of GeCl$_4$ (40.0 μL, 0.542 mmol). The initial dark-red solution was stirred for 1 h to give a clear red solution. The solvent was then removed under vacuo, and 10 mL of hexanes was used to extract product from the residue. The extract was then filtered through a 3 cm plug of silica gel, and the solvent was removed to give **9** as a red oil (0.094 g, 70%). ^{1}H NMR (400 MHz, CDCl$_3$): δ 7.07 (s, 2H, thienyl-H), 2.72 (m, 4H, -CH$_2$-), 2.59 (t, $^3J_{HH}$ = 7.2 Hz, 4H, -CH$_2$-), 1,78 (m, 4H, -CH$_2$-), 1.61 (pentet, $^3J_{HH}$ = 7.2 Hz, 4H, -CH$_2$-), 1.34 (m, 12H, -CH$_2$CH$_2$CH$_2$-), 0.90 (m, 6H, -CH$_3$). ^{13}C{^{1}H}NMR (100 MHz, CDCl$_3$): δ 144.1, 142.7, 137.6, 130.0, 122.5, 112.1, 31.7, 29.6, 29.5, 29.3, 28.9, 22.7, 22.3, 14.1. UV-vis (hexanes, nm, log ε): 453, 4.52.

Preparation of diethylgermole-2,5-di(2-bromro-3-hexylthiophenyl)(CH$_2$)$_4$ (10). To a solution of **9** (112 mg, 0.152 mmol) in 2 mL of THF was added CH$_3$CH$_2$MgCl (154 μL, 2.0 M solution in Et$_2$O, 0.30 mmol). The mixture was allowed to stir at room temperature overnight. After removing the solvent, 5 mL of hexanes was used to extract the product, and the crude product was then subjected to flash column chromatography (silica gel, hexanes), which yielded **10** as a red oil (18 mg, 20%). ^{1}H NMR (400 MHz, CDCl$_3$): δ 6.58 (s, 2H, thienyl-H), 2.68 (m, 4H, -CH$_2$), 2.55 (t, $^3J_{HH}$ = 7.6 Hz, 4H, -CH$_2$-), 1.74 (m, 4H, -CH$_2$-), 1.59 (pentet, $^3J_{HH}$ = 7.6 Hz, 4H, -CH$_2$-), 1.33 (m, 12H, -CH$_2$CH$_2$CH$_2$-), 1.20 (m, 4H, GeC*H$_2$*CH$_3$), 1.01 (t, $^3J_{HH}$ = 7.6 Hz, 6H, GeCH$_2$C*H$_3$*), 0.90 (m, 6H, -CH$_3$). ^{13}C{^{1}H}NMR (100 MHz, CDCl$_3$): δ 148.0, 143.4 (Ge-*C*=*C*-), 141.8, 130.0, 127.1, 108.8 (thiophene), 31.7, 30.5, 29.7, 29.4, 28.9, 23.2, 22.7, 14.1 (hexyl, and two −CH$_2$-), 9.1, 8.2

(ethyl). UV-vis (hexanes, nm, log ϵ): 312, 3.3. HR-MS (MALDI-TOF): m/z; Calcd. 726.06080. Found: 726.06097 (Δ ppm = 0.69).

Preparation of Compound 2,5-di(2-bromo-3-hexylthiophen-2-yl)selenophene(CH$_2$)$_4$ (12). To a solution of **8** (0.15g, 0.17 mmol) in 4 mL THF, was added a solution of freshly prepared SeCl$_2$ (0.17 mmol in 0.34 mL THF) by syringe. The color of the solution turned orange from its original dark-red color. The solution was allowed to stir at room temperature for 14 h in the absence of light. The solvent was removed under vacuum, and 5 mL of hexanes was used to extract product. The extract was then filtered through a 2 cm plug of silica gel. The solvent was removed from the filtrate to give **12** as a brown solid. ^{1}H NMR (400 MHz, CDCl$_3$): δ 6.79 (s, 2H, thienyl-H), 2.75 (t, $^3J_{HH}$ = 4.0 Hz, 4H, -CH$_2$), 2.55 (t, $^3J_{HH}$ = 4.0 Hz, 4H, -CH$_2$), 1.76 (t, $^3J_{HH}$ = 4 Hz, 4H, -CH$_2$), 1.60 (m, 4H, -CH$_2$), 1.34 (m, 12H, -CH$_2$CH$_2$CH$_2$), 0.89 (m, 6H, -CH$_3$). ^{13}C{^{1}H}NMR (100 MHz, CDCl$_3$): δ 142.5, 138.2, 137.8, 132.8, 126.5, 109.0, 31.7, 29.7, 29.6, 29.0, 28.8, 23.0, 22.7, 14.1. Compound **12** was thermally unstable at room temperature and decomposed both in solution and the solid state after 2 h to give an insoluble back solid. We were unable to obtain further characterization.

Preparation of 1,8-di(3-hexylthiophen-2-yl)octa-1,7-diyne (13). This compound was synthesized following the same procedure as for compound **7**. Using 2-bromo-3-hexylthiophene (3.12g, 12.6 mmol), 1,7-octadiyne (0.44 g, 4.2 mmol), Pd(PPh$_3$)$_4$ (242 mg, 0.21 mmol), CuI (45 mg, 0.21 mmol) as reagents, and 80 mL of THF and 30 mL diisopropylamine as solvents. The product was obtained as a pale yellow oil (1.00 g,

54%). ^{1}H NMR (400 MHz, CDCl$_3$): δ 7.06 (d, $^3J_{HH}$ = 5.2 Hz, 2H, thienyl-H), 6.82 (d,

$^3J_{HH}$ = 5.2 Hz, 2H, thienyl-H), 2.66 (t, $^3J_{HH}$ = 7.2 Hz, 4H, -CH$_2$-), 2.52 (m, 4H, -CH$_2$-),

1.79 (m, 4H, -CH$_2$-), 1.60 (pentet, $^3J_{HH}$ = 7.2, 4H, -CH$_2$- in hexyl), 1.30 (m, 12H, -

CH$_2$CH$_2$CH$_2$-, hexyl), 0.88 (m, 6H, -CH$_3$, hexyl). ^{13}C{^{1}H}NMR (100 MHz, CDCl$_3$): δ

146.7, 128.0, 124.5, 119.0 (thiophene), 95.7, 73.8 (C≡C), 31.7, 30.3, 29.4, 29.0, 27.8,

22.7, 19.4, 14.2. HR-MS (EI): m/z; Calcd. 438.24149. Found: 438.24125 (Δ ppm = -1.5).

Anal. Calcd. for C$_{28}$H$_{38}$S$_2$: C, 76.65; H, 8.73; S, 14.62. Found: C, 76.63; H, 8.75; S, 14.27.

Preparation of Cp$_2$Zr-2,5-bis(3-hexylthiophenyl)(CH$_2$)$_4$ (14). Compound **13** (0.50 g,

1.14 mmol) and Cp$_2$Zr(pyr)(Me$_3$SiC≡CSiMe$_3$) (0.54 g, 1.14mmol) were dissolved in 10

mL THF, and the resulting mixture was allowed to stir for 3 days to give a dark red

solution. The solvent was removed under reduced pressure, and the residue was extracted

with hexanes (2 x 3 mL). The extracted portion was filtered through Celite and cooling of

the filtrate to -30 °C resulted in the formation of **14** as dark red crystals (0.51g, 69%)

after 24 h. ^{1}H NMR (400 MHz, CDCl$_3$): δ 7.02 (d, $^3J_{HH}$ = 5.2 Hz, 2H, thienyl-H), 6.92 (d,

$^3J_{HH}$ = 5.2 Hz, 2H, thienyl-H), 6.27 (s, 10H, Cp), 2.48 (t, $^3J_{HH}$ = 8.0 Hz, 4H, -CH$_2$-), 2.02

(t, $^3J_{HH}$ = 6.8 Hz, 4H, -CH$_2$-), 1.69 (m, 4H, -CH$_2$-), 1.52 (pentet, $^3J_{HH}$ = 3.2 Hz, 4H, CH$_2$),

1.46 (m, 4H, -CH$_2$-), 1.37 (m, 8H, -CH$_2$CH$_2$-), 0.88 (m, 6H, -CH$_3$). ^{13}C{^{1}H}NMR (100

MHz, CDCl$_3$): δ 177.1 (Zr-*C*=C), 146.0 (Zr-C=*C*), 141.0, 130.7, 128.4, 120.9 (thiophene),

112.2 (Cp), 32.0, 30.8, 30.0, 29.4, 27.8, 22.7, 21.6, 14.2. UV-vis (hexanes, nm, log ϵ):

382, 4.11. Anal. Calcd for C$_{38}$H$_{48}$S$_2$Zr: C, 69.14; H, 7.33; S, 9.71. Found: C, 67.86; H,

7.22; S, 9.15.

Preparation of Compound 2,5-di(4-hexylthiophen-2-yl)selenophene(CH$_2$)$_4$ (15).

Freshly prepared SeCl$_2$ (0.37 mmol in 0.74 mL THF) was added to a solution of **14** (0.247 g, 0.37 mmol) in 5 mL of THF. The solution turned orange immediately after the addition of SeCl$_2$ and the reaction mixture was allowed to stir at room temperature for 14 h. The solvent was then removed under vacuum, and the product was extracted from the resulting solid using hexanes (2 x 3 mL). The combined extracts were then filtered through a 3 cm plug of silica gel. After the solvent was removed, the **15** was obtained as a yellow oil (0.12 g, 64%). ^{1}H NMR (400 MHz, CDCl$_3$): δ 7.27 (d, $^3J_{HH}$ = 2.0 Hz, 2H, thienyl-H), 6.96 (d, $^3J_{HH}$ = 5.2 Hz, 2H, thienyl-H), 2.58 (t, $^3J_{HH}$ = 7.6 Hz, 4H, -CH$_2$-), 2.559 (m, 4H, -CH$_2$-) 1.69 (m, 4H, -CH$_2$-), 1.58 (pentet, $^3J_{HH}$ = 7.6 Hz, 4H, -CH$_2$-), 1.27 (m, 12H, -CH$_2$CH$_2$CH$_2$-), 0.86 (m, 6H, -CH$_3$). 13C{1H}NMR (100 MHz, CDCl3): δ 141.5, 140.0 (Se-C=C-), 133.7, 131.1, 128.8, 125.0 (thiophene), 31.7, 30.7, 29.1, 29.0, 27.8, 23.2, 22.6, 14.1. UV-vis (hexanes, nm, log ε): 238,4.08; 283, 4.04. HR-MS (EI): m/z; Calcd. 518.15802. Found: 518.15792 (Δ ppm = 0.2). Anal. Calcd. for C$_{28}$H$_{38}$S$_2$Se : C, 64.96; H, 7.40; S, 12.39. Found: C, 64.00; H, 7.35; S, 12.00.

Preparation of 2,5-di(2-bromo-4-hexylthiophen-2-yl)selenophene(CH$_2$)$_4$ (16). To a solution of **15** (0.15 g, 0.28 mmol) in 5 mL of THF was added a solution of N-bromosuccinimide (0.10 g, 0.56 mmol) in 5 mL of THF at 0 °C. The resulting mixture was then warmed to room temperature and stirred for 12 h. Hexanes (50 mL) was then added to the mixture, and the combined organic fractions were washed with 30 mL of 10% Na$_2$S$_2$O$_3$, water, and then dried over MgSO$_4$. The volatiles were then removed from the solution to afford **16** as a yellow viscous oil (0.13 g, 69%). ^{1}H NMR (400 MHz, CDCl$_3$):

δ 6.91 (s, 2H, thienyl-H) 2.55 (m, 4H, -CH$_2$-), 2.51 (t, $^3J_{HH}$ = 7.6 Hz, 4H, -CH$_2$-), 1.68 (m, 4H, -CH$_2$-), 1.53 (pentet, $^3J_{HH}$ = 7.2 Hz , 4H, -CH$_2$-), 1.25 (m, 12H, -CH$_2$CH$_2$CH$_2$-), 0.87 (t, $^3J_{HH}$ = 6.8 Hz, 6H, -CH$_3$). ^{13}C{^{1}H}NMR (100 MHz, CDCl$_3$): δ 142.4, 140.7 (Se-C=C-), 132.9, 132.4, 131.6, 111.7 (thiophene), 31.6, 30.5, 29.0, 28.9, 27.8, 23.1, 22.6, 14.1. HR-MS (MALDI): m/z; Calcd. 675.97657. Found: 675.97609 (Δ ppm = 0.85). Anal. Calcd. for C$_{28}$H$_{36}$S$_2$Br$_2$Se: C, 49.70; H, 5.37; S, 9.49. Found: C, 49.32; H, 5.35; S, 9.24.

Preparation of Compound 1,3-bis(5-bromo-3-hexylthiophen-2-yl)selenophene(CH$_2$)$_4$ (17). To a solution of **14** (0.25g, 0.38 mmol) in 10 mL of THF was added HCl (1.0 mL, 2.0 M aqueous solution, 2.0 mmol). The dark red color of **14** immediately disappeared to give a colorless solution. After string for 5 min., distilled water (20 mL) was then added to resulting mixture, and the product was extracted with 30 mL of hexanes. The solvent was removed from the organic layer, and the crude product was purified by flash column chromatography (silica gel, hexanes) to give pure **17** as a pale yellow oil (0.15 g, 90 %). ^{1}H NMR (400 MHz, CDCl$_3$): δ 7.21 (d, $^3J_{HH}$ = 5.2 Hz, 2H, thienyl-H), 6.93 (d, $^3J_{HH}$ = 5.2 Hz, 2H, thienyl-H), 6.74 (t, $^4J_{HH}$ = 1.6 Hz, 2H, C=CH), 2.70 (m, 4H, -C=C-CH_2-) 2.64 (t, $^3J_{HH}$ = 7.6 Hz, 4H, -CH$_2$-), 1.73 (m, 4H, -C=C-CH$_2$-CH_2), 1.61 (pentet, $^3J_{HH}$ = 7.6 Hz, 4H, CH$_2$), 1.31 (m, 12H,- CH$_2$CH$_2$CH$_2$-), 0.87 (m, 6H, -CH$_3$). UV-vis (hexanes, nm, log ε): 331, 4.63. HR-MS (EI): m/z; Calcd. 440.25714. Found: 440.25760 (Δ ppm = 1.0). Anal. Calcd. for C$_{28}$H$_{40}$S$_2$: C, 76.30; H, 9.15; S, 14.55. Found: C, 76.45; H, 9.32; S, 13.37.

Preparation of PM3 from the polymerization of 16 A solution of Ni(COD)$_2$ (121 mg, 0.44 mmol) and bipyridine (65 mg, 0.44 mmol) in 5 mL toluene was heated to 80 °C for 1 h. Subsequently, **16** (0.107 g, 0.158 mmol) was added as a solution in 5 mL of toluene

under N_2. Upon the addition of **16**, the color of the solution gradually became dark green. After stirring at room temperature for 20 h, 30 mL THF of was added, and the mixture was stirred for a further 1 h. The polymer was isolated by precipitating the solution into 300 mL of rapidly-stirring MeOH and isolated by filtration and dried to obtain **PM 3** (70 mg, 86%) UV-vis (THF, nm, log ϵ): 382, 4.52.

Table 2.1 Crystallographic data forcCompounds **8** and **14**

	8	14
empirical formula	$C_{38}H_{46}Br_2S_2Zr$	$C_{38}H_{48}S_2Zr$
fw	817.91	660.10
cryst dimens (mm^3)	0.23 x 0.08 x 0.08	0.18 x 0.09 x 0.08
cryst syst	triclinic	monoclinic
space group	$P\bar{1}$ (No. 2)	$C2/c$ (No. 15)
unit cell dimensions		
a (Å)	12.2864(6)	37.7722 (5)
b (Å)	12.4938 (6)	9.0101 (1)
c (Å)	12.9530 (6)	20.3354 (3)
α (deg)	75.5839(6)	
β (deg)	67.1067 (6)	100.1582 (7)
γ (deg)	74.8353(6)	
V (Å^3)	1743.54(14)	6812.29 (15)
Z	2	8
ρ (g cm^{-3})	1.558	1.287
abs coeff (mm^{-1})	2.753	3.956
T (K)	173(1)	173(1)
$2\theta_{max}$ (deg)	55.20	54.98
total data	15628	22309
unique data (R_{int})	7257 (0.0946)	9835 (0.0143)
obs data [$I > 2\sigma(I)$]	8025	6336
Params	388	370
R_1 [$I > 2\sigma(I)$][a]	0.0364	0.0320
wR_2 [all data][a]	0.0817	0.0876

[a]Obtained from least-squares refinement of 9531 reflections with $8.84° < 2\theta < 139.02°$.

2.5 References

[1] Brabec, C. J.; Dyakonov, V.; Scherf, U. In *Organic Photovoltaic: Materials, Device Physics, and Manufacturing;, John Wiley & Sons: 2008.*

[2] (a) Xin, H.; Kim, F. S.; Jenekhe, S. A. *J. Am. Chem. Soc.* **2008**, *130*, 5424. (b) Lee, J. K.; Ma, W.; Brabec, C. J.; Yuen, J.; Moon, J. S.; Kim, J. Y.; Lee, K.; Bazan, G. C.; Heeger, A. *J. Am. Chem. Soc.* **2008**, *130*, 3619.

[3] Beaujuge, P. M.; Subbiah, J.; Choudhury, K. R.; Elliger, S.; McCarley, T. D.; So, F.; Reynolds, J. R. *Chem. Mater.* **2010**, *22*, 2093.

[4] Kim, Y.; Cook, S.; Tuladhar, S. M.; Choulis, S. A.; Nelson, J.; Durrant, J. R.; Bradley, D. D. C.; Giles, M.; McCulloch, I.; Ha, C.-S.; Ree, M. *Nat. Mater.* **2006**, *5*, 197.

[5] (a) Das, S.; Zade, S. S. *Chem. Commun*. **2010**, *46*, 1168. (b) Das, S.; Bedi, A.; Krishna, G. R.; Reddy C. M.; Zade, S. S. *Org. Biomol. Chem.* **2011**, *9*, 6963.

[6] Hay, C.; Fave, C.; Hissler, M.; Rault-Berthelot, J.; Réau, R. *Org. Lett.* **2003**, *5*, 3467.

[7] Fagan, P. J.; Nugent, W. A.; Calabrese, J. C. *J. Am. Chem. Soc*. **1994**,*116,* 1880.

[8] Mao, S. S. H.; Tilley, T. D. *Macromolecules* **1997**, *30*, 5566.

[9] Luch, L. B.; Mao, S. S. H.; Tilley, T. D. *J. Am. Chem. Soc*. **1998**, *120*, 4354.

[10] Mao, S. S. H.; Tilley. T. D. *J. Am. Chem. Soc*. **1995**, *117*, 5365.

[11] Johnson, S. A.; Liu, F.; Suh, M. C.; Zurcher, S.; Haufe, M.; Mao, S. H.; Tilley, T. D. *J. Am. Chem. Soc.* **2003**, *125*, 4199.

[12] Miller, D. A.; Liu, F. J.; Jonson, S. A.; Lee, H.; McBee, L. J; Tilley, T. D. *J. Am. Chem. Soc.* **2009**, *131*, 4117.

[13] (a) Brown, P. J.; Thomas, D. S.; Kohler, A.; Wilson, J. S.; Kim, J. S.; Ramsdale, C. M. *Phys. Rev. B* **2003**, *67*, 64203. (b) Sirringhaus, H.; Brown, P. J. Friend, R. H.; Nielsen, M. M.; Bechgaard, M. M.; Langeveld-Voss, B. M. W.; Spiering, A. J. H.; Jassen, R. A. J.; Meijer, E. W.; Herwig, P.; de Leeuw, D. M. *Nature* **1999**, *401*, 685.

[14] Jiang, B.; Tilley, D. T. *J. Am. Chem. Soc.* **1999**, *121*, 9744. (b) Fave, C.; Hissler, M.; Réau, R. *J. Am. Chem. Soc.* **2004**, *126*, 6058.

[15] Nitschke, J. R.; Zuercher, S.; Tilley, T. D. *J. Am. Chem. Soc.* **2000**, *122*, 10345.

[16] Chen, H.-Y.; Hou, J.; Hayden, A. E.; Yang, H.; Houk, K. N.;Yang, Y. *Adv. Mater.* **2010**, *22*, 371.

[17] Scharber, M. C.; Koppe, M.; Gao, J.; Cordella, F.; Loi, M. A.; Denk, P.; Morana, M.; Egelhaaf, H.-J.; Forberich, K.; Dennler, G.; Gaudiana, R.; Waller, D.; Zhu, Z.; Shi, X.; Brabec, C. J. *Adv. Mater.* **2010**, *22*, 367.

[18] Gendron, D.; Morin, P.-O.; Berrouard, P.; Allard, N.; Aïch, B. R.; Garon, C. N.; Tao, Y.; Leclerc, M. *Macromolecules* **2011**, *44*, 7188.

[19] Yamaguchi, S.; Itami, Y.; Tamao, K. *Organometallics* **1998**, *17*, 4910.

[20] Ura, Y.; Li, Y.; Xi, Z.; Takahashi, T. *Tetrahedron Lett.* **1998**, *39*, 2787.

[21] Pangborn, A. B.; Giardello, M. A.; Grubbs, R. H.; Rosen, R. K.; Timmers, F. J. *Organometallics* **1996**, *15*, 1518.

[22] (a) Rosenthal, U.; Ohff, A.; Baumann, W.; Tillack, A. Z. *Anorg, Allg, Chem.* **1995**, *621*, 77. (b) Nguyen, H. T.; Coulembier, O.; Winter, J. D. *Polym. Bull.* **2011**, *66*, 51.

Chapter 3: Summary and Future Work

3.1 Summary

We have developed a novel synthetic route for the preparation of conjugated polymers. Compared with many pre-existing routes, convenience and tunability of band gaps via zirconium-mediated metallacycle transfer are the most remarkable features of this method. One conjugated polymer consisting of alternating thiophene/selenophene was successfully prepared using this synthetic route. The optical and thermal properties have been studied which demonstrated that the presence of Se in a conjugated polymer leads to lower optical band gap when compared to a monomeric analogue.

3.2 Future research directions towards the synthesis of conjugated polymers via metallacycle transfer chemistry

The synthetic route developed in this Thesis will be useful for future synthetic efforts that aim to incorporate other main group heteroles into conjugated polymers, which previously required lengthy synthetic pathways. Even though one successful example (**PM3** in Chapter 2) has demonstrated the utility of this synthetic route, the versatility of the metallacycle transfer chemistry in this synthetic route has not been fully studied. It is certainly worthy to devote time to expand the scope of this transformation to prepare new inorganic polymers, particularly those containing heavy main group elements (Scheme 3.1). It is of interest to ascertain how the presence of different heavy main group elements can affect electronic and optical properties of conjugated polymers since studies in this area still somewhat rare.[1]

E = heavy main group elements
such as Ge, Sn, Te

X = halides
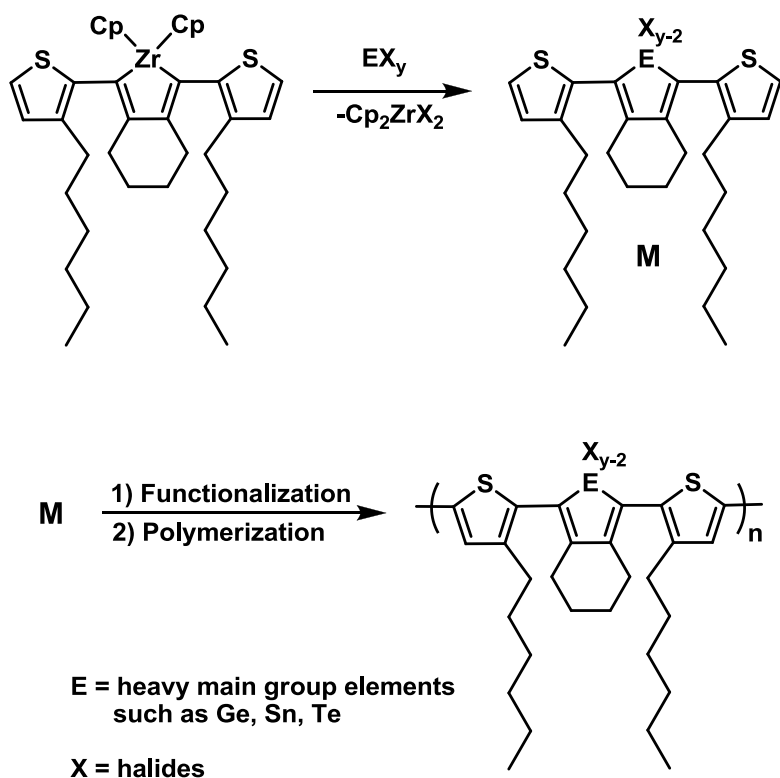
Scheme 3.1 Synthesis of conjugated polymers containing heavy main heteroles.

3.3 Improving the synthetic route toward conjugated polymers via Suzuki cross-coupling

After reviewing each step in our synthetic route, we have noticed that the Pd(0) catalyzed cross-coupling reactions between halogenated thiophene and 1,7-octadiyne gives quite low product yields; meanwhile, this reaction also requires sophisticated control over reaction conditions and separation of the product from excess halogenated thiophene by column chromatography. It would be beneficial for future research if we can replace Pd(0) catalyzed cross-coupling reactions, such as the Sonagashira coupling routes used in Chapter 2, with other simple, high yielding reactions.[2]

Therefore, we propose a modified synthetic route by using 4,4,5,5-tetramethyl-1,3,2-dioxaborolane (**BPin**) (Scheme 3.2). The **BPin**-capped diyne **1** can be rapidly prepared in high yield, and following similar chemistry performed in Chapter 2, we should be able to obtain a series of **BPin**-terminated main group heteroles (**M1-M4**). Finally, polymers should be readily formed via well-known, high yielding Suzuki coupling with halogenated aryl groups.

i) ^{n}BuLi, THF, 1 h, 0 ^{o}C; ii) Isopropylpinacol borate, 12 h;
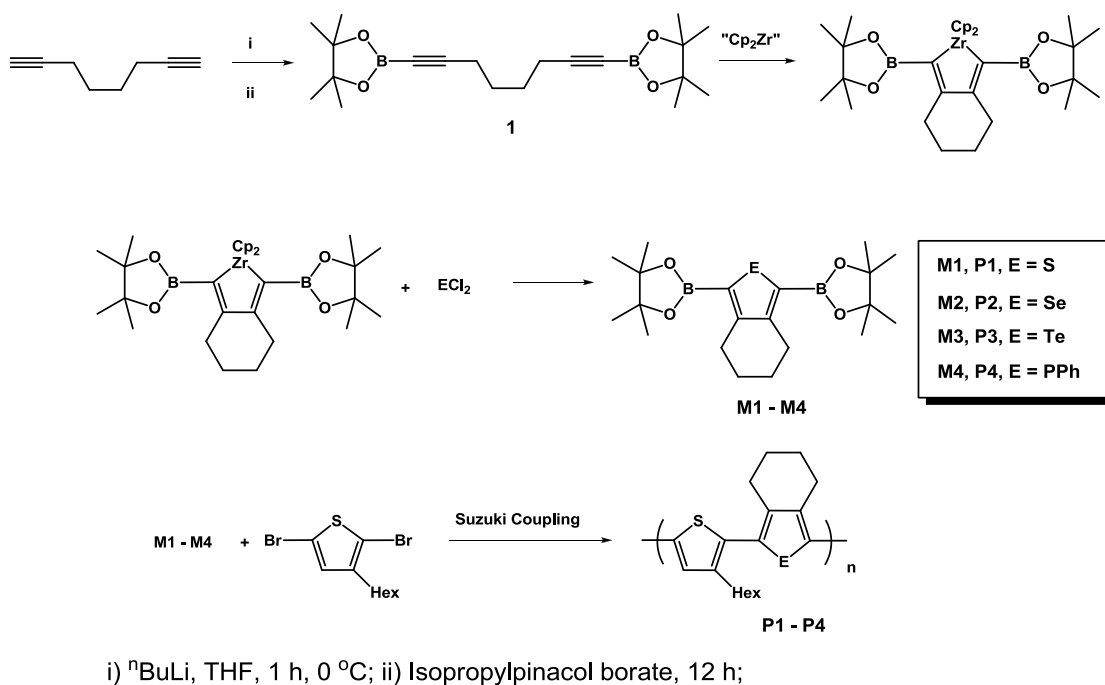
Scheme 3.2 Synthesis of conjugated polymers via **BPin**-terminated diynes.

3.4 References

[1] McCormick, T. M.; Jahnke, A. A.; Lough, A. J.; Seferos, D. S. *J. Am. Chem. Soc.* **2012**, *134*, 3542.

[2] Gandon, v.; Leca, D; Aechtner, T.; Malacrla, M; Auberta, C. *Org. Lett.* **2004**, *6*, 3405.